Proposal for a X-FEL User Consortium for the HELMHOLTZ-BEAMLINE at the European XFEL

19. March 2012

The HELMHOLTZ-BEAMLINE at the European XFEL will establish multi-purpose high-power and ultra-intense lasers as well as high-field magnets at the SASE2 end-station of the European XFEL. This will constitute a world-wide unique combination of ultra-high power lasers and high-field magnets with a high-brilliance X-ray source. It will extend the scope of research that can be carried out at the European XFEL beyond the baseline Instruments, especially in the areas of strong-field physics, high energy density science, relativistic laser-plasma physics, ultra high-pressure astro- and planetary-physics, dynamic materials research, and magnetic phenomena in condensed matter. The laser systems will include: an ultra-intense PW-class laser operating with full energy at 1 Hz, and at 200 TW at 10 Hz, based either on emerging diode-pumped solid-state laser technology, or on commercially available Ti:Sapphire technology; a high energy kJ-class laser with few ns-duration shaped pulses for shot-on-demand operation, with a 100 J-class stage operating at 1 Hz; and a 1.5 MJ pulse generator to drive pulsed high-field magnets (50 T, ~1ms) for condensed matter and magnetized HED-plasma research. The HELMHOLTZ-BEAMLINE will be used to drive matter to extremes of temperature, density, pressure, field strength, and/or particle irradiation, which can be probed with the XFEL beams; or alternatively to probe XFEL-driven samples with laser-generated particles or radiation. The HELMHOLTZ-BEAMLINE is being proposed for funding from the Helmholtz Association research area “Matter,” by partners HZDR, DESY and HI-Jena. Over 80 research groups from more than 60 institutions in 15 countries have joined this User Consortium as External Partners.

Representative:

Prof. Dr. Thomas Cowan
Helmholtz-Zentrum Dresden-Rossendorf (HZDR)
Institute of Radiation Physics
Bautzner Landstrasse 400
D-01314 Dresden
E-mail: t.cowan@hzdr.de
Phone: +49-351-260-2270 (Fax: -3700)

Key Scientists (Helmholtz)

Prof. Dr. Ulrich Schramm
HZDR, Institute of Radiation Physics
Bautzner Landstrasse 400
D-01314 Dresden
E-mail: u.schramm@hzdr.de
Phone: +49-351-260-2471 (Fax: -12471)

Prof. Dr. Edgar Weckert
Forschung mit Photonen DESY
Notkestr. 85
D-22603 Hamburg
Email: edgar.weckert@desy.de
Phone: +49 (0)40-8998-4509 (Fax: -4475)

Prof. Dr. Thomas Stoehlker
Helmholtz-Institute Jena
Fröbelstieg 3
D-07743 Jena
Email: t.stoehlker@gsi.de
Phone: +49 (0)3641-947-603 (Fax: -602)

Extended Membership:

The Scientific Case for the HELMHOLTZ-BEAMLINE has been developed with broad support from Universities and Research Institutes in Germany, across Europe, and from Asia and North America.

Present partners at German Universities and Research Institutes

Centre for Free-Electron Laser Science, CFEL/DESY

Dr. A. Barty & coworkers

DESY, Hamburg

Prof. E. Weckart & coworkers, (Photon Science and HASYLAB)
Dr. S. Toleikis, Dr. M. Harmand, Dr. S. Dusterer et al (FLASH-WDM Group),
Dr. H.-P. Liermann (Extreme Conditions), Dr. H. Franz (Nucl. Res. Scatt.),
Dr. J. Strempfer, Dr. M. v. Zimmermann (Magnetism and Correlated Electrons)

ExtreMe Matter Institute, EMMI-GSI

Dr. P. Neumayer; Dr. A. Gumberidze

GFZ - Deutsches GeoForschungsZentrum Potsdam

Prof. W. Heinrich & coworkers.

GSI - Darmstadt

Dr. V. Bagnoud, Prof. Th. Kühl, Dr. U. Eisenbarth, Dr. S. Götte, Dr. A. Blazevic,
Dr. A. Tauschwitz, Dr. O. Rosmej, Dr. K. Weyrich, Dr. W. Quint

Helmholtz-Institut Jena (HIJ)

Prof. T. Stoehlker, Dr. G. Weber, Dr. R. Märtin, Dr. E. Förster, Dr. O. Jäckel,
Dr. R. Bödefeld, Dr. B. Zielbauer, Dr. S. Trotsenko, M. Hornung, F. Karbstein

Helmholtz-Zentrum Dresden-Rossendorf (HZDR)

Prof. T. Cowan, Prof. U. Schramm, Prof. B. Kaempfer, Prof. R. Sauerbrey,
Dr. M. Bussmann, Dr. S. Kraft, Dr. M. Siebold et al (Laser Part. Accel)
Dr. K. Fahmy et al (Biophysics Group), Dr. M. Gensch et al (THz Group)
Dr. J. Grenzer, Dr. M. Posselt et al. (Inst. Ion Beam Phys & Mat Res)
Dr. T. Herrmannsdoerfer et al. (High- magnetic-field Lab Dresden, HLD)

Max Born Institute Berlin

Prof. W. Sandner, Prof. M. Schnürer & coworkers

Max-Planck-Institut für Kernphysik

Prof. C.H. Keitel, Dr. A. Palffy, PD Dr. K.Z. Hatsagortsyan, PD Dr. A. Di Piazza

Max-Planck-Institut für Quantenoptik (MPQ)

Dr. Z. Major

OncoRay, Gustav Carus Medizinsches Fakultät, TU Dresden

Prof. N. Cordes, Prof. A. Dubrovsky

Universität Bayreuth

Prof. Dr. L. Dubrovinsky & coworkers (Bayerisches Geoinstitut)

Technische Universität Darmstadt

Prof. M. Roth & coworkers (Institut für Kernphysik)

Technische Universität Dresden

Prof. Dr. C. Schroer & coworkers (Institut für Strukturphysik).

Universität Frankfurt am Main

Prof. B. Winkler & coworkers (Institut für Geowissenschaften)

Albert-Ludwigs-Universität Freiburg

Prof. Th. Kenkmann & coworkers (Institut für Geowissenchaften)

Friedrich-Schiller-Universität Jena

Prof. H. Gies & coworkers (Theor. Physik. Inst.)
Prof. G. Paulus, Prof. M. Kaluza, Dr. I. Uschmann & coworkers (IOQ-Jena)

Ludwig Maximilian-University, Munich (LMU)

Prof. H. Ruhl, Dr. N. Elkina, Dr. C. Klier & coworkers
Prof. S. Karsch & coworkers

Universität Rostock

Prof. Dr. R. Redmer & coworkers

University of Siegen

Prof. Dr. U. Pietsch & coworkers

Present European and other Partners

CH: Paul-Scherrer-Institute

Dr. A. Froideval, Dr. J. Bertsch, Dr. J. Chen, Dr. C. Degueldre, Dr. M. Krack, Dr. G. Kuri, Dr. M. Martin, Dr. S. Portier, Dr. M. A. Pouchon, Dr. F. Devynck, Dr. I. Lund

CZ: FZU - Insitute of Physics, Academy of Science of Czech Republic

Prof. G. Korn, Prof. J. Krasa, Prof. B. Rus, Dr. D. Margarone & ELI-Beamlines Team

ES: CLPU – Centro de Laseres Pulsados Ultracortos Ultraintensos, Univ. of Salamanca

Prof. L. Roso, Dr. R. Torres & coworkers

FR: IRAMIS, CEA, Saclay

Prof. H. Merdji & coworkers (Service des Photons, Atomes et Molécules)

CEA, Arpajon

Prof. P. Lobeyre & coworkers (High Pressure Group)

LULI, Ecole Polytechnique–CNRS–CEA-UPMC

Dr. P. Audebert, Dr. S. Baton, Dr. J. Fuchs & coworkers (ELFIE group)
Dr. M. Koenig & coworkers (High Energy Density group)

CELIA (Centre Lasers Intense et Applications), Universite Bordeaux

Prof. D. Batani, Dr. F. Dorchies, Dr. J.J. Santos & coworkers
Prof. V. Tikhonchuk, Dr. E. d'Humieres & coworkers

Universite Sorbonne, Universite Pierre et Marie Curie (UPMC)

Prof. F. Rosmej, Dr. P. Angelo, Dr. K. Bennadji & coworkers.

HU: University of Pecs, Institute of Physics

Prof. J. Hebling, Prof. J. A. Fulop

IT: SAPIENZA Unviersity of Roma

Prof. L. Palumbo, Dr. L. Lancia, Dr. P. Antici

PL: Military University of Technology, Warsaw

Prof. H. Fiedorowicz & coworkers (Institute of Optoelectronics)

RU: Joint Institute for High Temperatures, Russian Academy of Sciences

Dr. S. Pikuz & coworkers

SE: Stockholm University
Prof. U. Häussermann & coworkers

Umea University
Prof. M. Marklund, Dr. A. Ilderton, Dr. Chris Harvey, A. Gonoskov

Uppsala University, Institute of Molecular Biophysics
Prof. J. Hajdu, Dr. J. Andreasson, Dr. N. Timneanu, Dr. M. Svenda, B. Iwan, & coworkers

UK: University of Edinburgh
Prof M. McMahon, Prof. R. Donovan, Dr. C. Murphy & coworkers.

Imperial College (IC)
Prof. S. Bland, Dr. D. Eakins & coworkers

Queens University Belfast (QUB), Centre for Plasma Physics
Prof. M. Borghesi, Prof. C. Lewis, Prof. D. Riley, Prof. M. Zepf, Dr. B. Dromey & coworkers

University College London (UCL)
Prof. P. McMillan, Dr. C. Pickard, Dr. F. Cora, Dr. M. Gillan, & coworkers

University of Oxford
Prof. J. Wark, Prof. G. Gregori & coworkers

University of Plymouth
Prof. T. Heinzl, Prof. D. McMullan, Dr. K. Langfeld, Dr. M. Lavelle, N. Iji, M. Raddadi

Scottish Universities Physics Alliance (SUPA)
Prof. K.D. Ledingham & coworkers (Nuclear Interactions at High Temperatures)

University of Strathclyde
Prof. D. Jaroszynski, Dr. S. Cipiccia, & coworkers

CN: Institute of Physics, Chinese Academy of Sciences (IOP-CAS)
Prof. Yutong Li & coworkers

Peking University (PKU)
Prof. Dr. Xueqing Yan & coworkers (Inst. of Heavy Ion Physics)

Shanghai Jiao Tong University (SJTU)
Prof. Zheng-Ming Sheng & coworkers

Shanghai Institute of Optics and Fine Mechanics (SIOM), Chinese Academy of Sciences
Prof. Ruxin Li & coworkers

IN: Tata Institute of Fundamental Research (TIFR)
Prof. G. Ravindra Kumar & coworkers

JP: Institute of Laser Engineering, ILE – Osaka University
Prof. H. Takabe, Dr. L. Baiotti, Dr. T. Moritaka (Theory)
Prof. Y. Sakawa, Prof. Y. Kuramitsu, Dr. T. Morita (Expt. Lab. Astrophys.)
Prof. A. Hosaka (Research Center for Nuclear Physics).
Prof. K. Mima (Fusion Materials)

Kansai Photon Science Institute (KPSI), JAEA
Prof. P. R. Bolton, and coworkers

Kyoto University, Institute for Chemical Research
Prof. S. Sakabe, & coworkers (Advanced Research Center for Beam Science)

US: Carnegie Institution of Washington
Prof. A. Goncharov & coworkers (Geophysical Laboratory)

General Atomics
Dr. R. Stephens, Dr. M-S Wei & coworkers

Los Alamos National Laboratory
Dr. K. Schoenberg, Dr. J. Sarrao, Dr. C. Barnes, Dr. J. Fernandez, Dr. M. Hegelich & coworkers

Lawrence Berkeley National Laboratory
Prof. R. W. Falcone, Dr. B.-I. Cho.

Lawrence Livermore National Laboratory
Dr. M. Armstrong (High Pressure Group); Dr. G. Collins et al (High Energy Density Section)
Dr. S. H. Glenzer et al (Plasma Physics Group), Dr. S. Hau-Riege et al (X-ray Group);
Dr. P. Patel et al (Fast Ignition-Fusion Energy Sciences Program);
Dr. R. Shepherd, Dr. H. Chen, Dr. R. Cauble et al. (Jupiter Laser Facility)

Oak Ridge National Laboratory, Materials Science and Technology Division
Dr. B. Larson (Senior Fellow), Dr. J. Tischler, Dr. G. Eres, Dr. Y. Osetskiy, Dr. G. Samolyuk, Dr. R. Stoller, Dr. S. Xu

Ohio State University, Department of Physics
Prof. R. R. Freeman & coworkers (High Energy Density Physics group)

The Rockefeller University
Prof. T. P. Sakmar, M.D.

SLAC National Accelerator Laboratory
Dr. R. Nagler, & coworkers (LCLS-MEC)

University of California, San Diego
Prof. F. Beg & coworkers (Dept. Mechanical & Aerospace Eng.)

University of Nevada, Reno
Prof. Y. Sentoku

European XFEL:

Dr. Thomas Tschentscher
Scientific Director
European XFEL GmbH
Notkestr. 85
D-22607 Hamburg
Email: thomas.tschentscher@xfel.eu
Phone: +49 (0)40-8998-3904 (Fax: -1905)

1 Executive Summary

The Helmholtz-Beamline will establish high-power and high-energy lasers and high-field pulsed magnets at the SASE2 end-station of the European XFEL. It will include: high repetition-rate PW-class laser beams (PW at 1 Hz; 200 TW at 10 Hz); shaped few ns, kJ-class laser pulses (kJ at "shot-on-demand," and 100 J at 1 Hz); and high-field (50 T) pulsed magnets. This will constitute a world-wide unique combination of ultra-high brilliance x-ray beams with ultra-intense lasers and strong fields. And it promises new scientific opportunities in high energy density science, relativistic laser-plasma research, strong-field physics, ultrafast dynamics in materials and complex systems, and magnetic phenomena in condensed matter.

The Helmholtz-Beamline will be coupled to the HED Instrument and will contribute to the study of High Energy Density states of matter, including the Equation of State of warm dense matter (WDM), phase transitions at high pressure, and dynamics of HED plasmas. New vistas will be opened for geophysics and planetary science, by extending the range of high pressure conditions accessible at hard x-rays sources up to 10 Mbar by cold ramped compression with the shaped ns-pulses. The high repetition rate of the lasers, and the outstanding XFEL beam characteristics, offer to transform the study of WDM and TPa-range of materials physics from an era of "demonstration" to one of precision and systematic exploration.

The unique combination ultra-bright x-ray beams with extreme strong-fields achievable in the focus of the ultra-intense PW laser, will open new venues in the fundamental study of classical and quantum electrodynamics. For example, the XFEL beam will be used to test QED predictions of vacuum polarization in in the strong field produced in the PW-laser focus.

New insight into the atomic-level processes and dynamics that occur in ion beam processing of electronic materials, or in extreme radiation environments, will be gained in ion-pump, XPCS-probe experiments of ion-collision cascades initiated by laser-accelerated particles. This will contribute towards a predictive understanding of the processing and performance of advanced materials.

X-ray Magnetic Absorption and Scattering in strong pulsed magnetic fields at XFEL will allow for unique experiments at the forefront of condensed-matter physics, with access to element selective information on band structure, spin, and orbital magnetic contributions. This will advance our knowledge of rare-earth high-temperature superconductors, strongly correlated electron systems, heavy-fermion materials, and spin-ice compounds with magnetic monopole excitations.

The unprecedented brightness of the XFEL x-ray beams will allow us peer inside of the solid-density plasma created during ultra-intense laser interactions with matter. This will help unravel the immensely complex fs-scale dynamics of relativistic electron transport at extremes of current density and electromagnetic field strength. This physics is central to many applications of high-intensity lasers, including high-gradient ion acceleration, ultrafast radiation generation, and isochoric heating, and will be a critical issue for next generation laser facilities which seek to surpass 10^{22} W/cm^2.

Following an initial workshop on PW Lasers at Hard X-ray Light Sources (Dresden, Sept 2011) with 70 participants from 25 institutions, the User Consortium membership has expanded to include more than 80 groups from over 60 institutions in 15 countries (with a potential scientific user community of more than 600 faculty, staff and research associates).

2. Science Case

The generation and study of matter at high energy density (HED) and under extreme conditions (MEC) of pressure, temperature and magnetic field, are rapidly growing areas of research, which reflects its importance in many diverse disciplines of fundamental and applied science. Among others, these include astrophysics, geophysics, planetary science, magnetism in condensed matter physics, high-T_c superconductivity, materials processing, high pressure physics and chemistry, fusion research, advanced accelerators, biophysics, ultrafast science, and all manner of laser-matter interactions and laser-plasma physics. Many expert studies have identified HED and MEC research as an important frontier in modern science and for technologies of tomorrow.[1,2]

HED and MEC science are a staple at large scale research facilities world-wide, including synchrotron light sources, laser-implosion facilities, high-energy particle accelerators, Z-machines, high-field magnet facilites, and x-ray FELs.[3,4] The Helmholtz-Beamline at the European XFEL will bring together in one location many aspects of these complementary capabilities, and bring to bear the unprecedented qualities of the European XFEL x-rays in terms of brightness, tunability, polarization, coherence, temporal resolution and high photon number per pulse. The scientific opportunities identified here do not only represent an extension of the parameter regimes that can be studied at the XFEL. They represent as well the major impact that the discovery potential afforded by the European XFEL can have on the scientific productivity of other fields and disciplines, including notably the physics possible with high-intensity lasers, and their further application.

2.1 High Energy Density States of Matter

2.1.1 Warm Dense Matter and Hot Dense Matter

The Scientific Case for WDM research at the European XFEL is well documented.[4] The XFEL beams will provide extraordinary new capabilities to produce and probe WDM states on ultrafast time scales, with isochoric x-ray heating, followed by isentropic relaxation (Fig. 2.1.1a). The PW laser capability will allow additional means to heat matter, including with laser-accelerated ions [5] and hot electrons, which are confined by self-generated magnetic [6] and electrostatic [7] fields, or by external pulsed magnetic fields [8]. Shock heating will be driven directly by laser-ablation-driven shocks (Fig 1b), as well as deep within a target by collisional shocks at the interface between buried layers heated by laser-generated hot electrons [9].

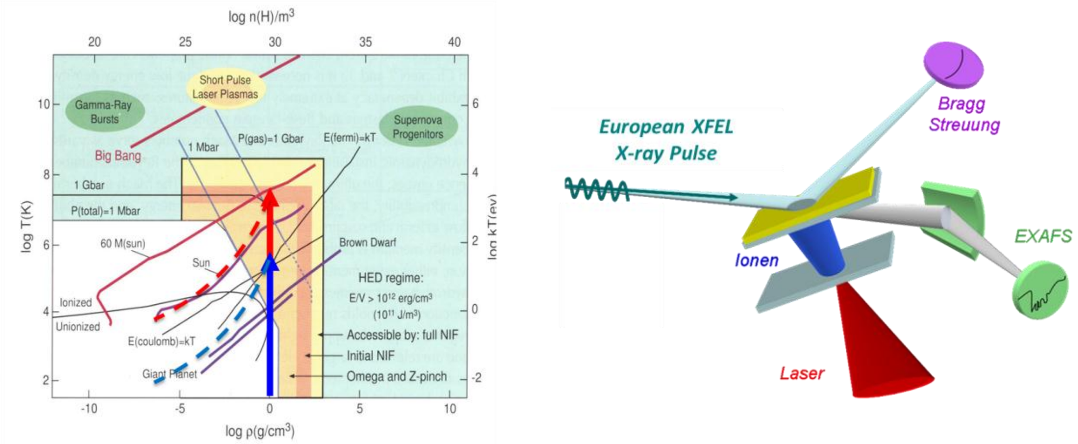

Figure 2.1.1: (a) left: T-ρ phase diagram of hydrogen, accessible by isochoric heating and isentropic expansion, with XFEL (blue) or PW laser (red). (b) right: Schematic of laser-ion-pump, XFEL-probe WDM experiment.

Each of these laser-based techniques has limitations for precision EOS determinations of HED states of matter, due to the often large spatial and temporal gradients. Studying these techniques at the European XFEL will allow single-shot characterization of the HED conditions precise temporal and spatial resolution, which will provide new insight into the non-thermal heating, energy transport and relaxation processes and timescales inherent in each. This understanding will help in the interpretation of experiments using these techniques, and further their application in HED research, at other laser-only facilities.

2.1.2 WDM in Planetary Science

A particularly exciting research area in high energy density science is physics of planetary interiors, which represent a perfect laboratory for high-pressure physics. Besides the eight Solar planets, hundreds of extrasolar planets have been detected since 1995 [12] and, due to space missions such as Corot and Kepler, thousands of new ones will be observed in the next years. In the past we have distinguished between terrestrial planets like the Earth, Mercury, Venus, and Mars, icy planets like Uranus and Neptune, and gaseous planets like Jupiter and Saturn. Due to the enormous progress in observational astronomy, new classes of planets like Super-Earths, Hot Jupiters, and Hot Neptunes have been identified [13].

The physical conditions in the interior of these planets cover a wide range of temperature (10^2-10^5 K) and pressure (1 bar-100 Mbar). The materials of interest are mostly hydrogen and helium, ices like CH4, NH3, OH2, rocky material of the Fe-Si-Mg-O complexes (perovskites, periclase, etc), as well as mixtures of all these species. Thus, planetary interiors offer not only a wide range of physical parameters to be studied, but also many classes of materials to be investigated. Fundamental properties such as the equation-of-state data and the phase diagram (for hydrogen, see e.g. [14,15]), nonmetal-to-metal transitions [16,17], and demixing phenomena [18] are relevant in this context since they are of paramount importance for state-of-the-art interior [19] and dynamo models [20]. However, relatively little data exist in this high-pressure regime. For instance, the melting line of the simplest element hydrogen is not well known above 1 Mbar [14] and that of iron -most important for the Earth's core and the interior structure of Super-Earths- is still under debate in the high-pressure domain [21]. Further problems are the existence of exotic phases such as superionic water [22,23] or the demixing region in the H-He system [24,25]. Although ab initio simulations (cf. Fig. 2.1.2) have a great predictive power, benchmarking experiments in the multi-Mbar regime of WDM are essential for the further progress of planetary sciences.

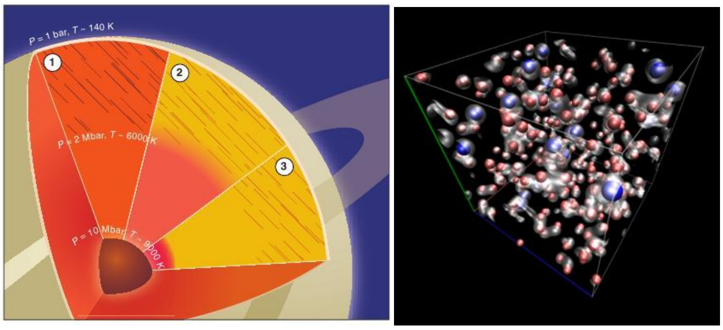

Figure 2.1.2: Left: Three views of Saturn's interior showing the H/He ratio, before the onset of He phase separation (1), and at present time using competing phase diagrams (2,3). **Right:** Simulation of warm dense H-He at Mbar pressures, showing isospheres of electron density).

2.1.3 Matter at Extreme Compression

Until recently, the traditional view of how matter behaved under high pressure was that all materials would trend towards high-symmetry, close-packed metallic phases, where the ionic cores would be surrounded by a sea of pressure-ionised valence electrons [28]. But recent advances in static compression science [29], and in *ab initio* computational theory and computation [30], have shown the true behaviour to be completely different – and much more interesting. Under compression, interactions between the core electrons on neighbouring atoms emerge, and at TPa pressures the gas-like valence electrons become localised in interstitial regions within the lattice, forming “electride” phases [30]. At least 23 elements have now been found to have complex structural forms at high pressure. Such phases are characterised by complex atomic structures in even “simple” metals such as Na [31], metal-insulator or metal-semiconductor transitions in alkali metals such as Li and Na, [32], and unusual melting behaviour [33,34]. Even aluminium is predicted to undergo a transition to a complex incommensurate form above 3.2 TPa (32 Mbar) – see Figure 2.1.3 [35], and this exotic behaviour has called for a paradigm shift in the understanding of how high-density matter behaves.

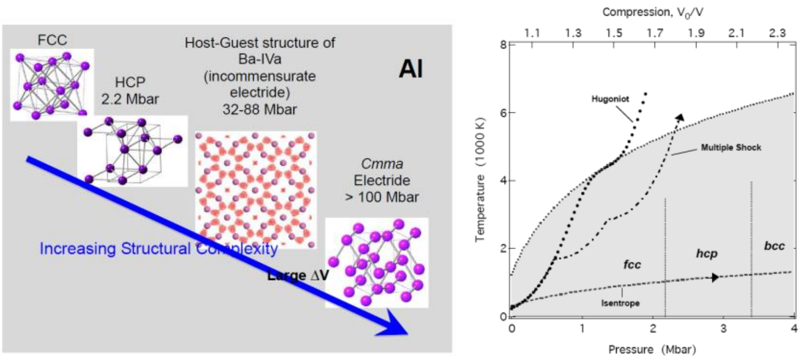

Figure 2.1.3: (a) Complex structures predicted to appear in Aluminium at ultra-high pressures (Refs. [35,37]). (b) Aluminum P-T conditions accessible by laser-driven shocks, isentropic compression with shaped ns-pulses.

The effect of how core electron interactions affect the physical properties of materials, such as strength, thermal conductivity and resistivity, is completely unknown. Recent results at NIF-scale pressures have shown unexpected new phases of materials at high compression, indicating exciting new physics, which if understood could lead to potentially new classes of materials. For example, a recent expert workshop report [36] concludes, “Compression of matter results in reordering of the shell structure of electronic levels in atoms, effectively creating a “new” periodic table with the promise of creating wholly new materials. When combined with the ability of using temperature to rearrange populations of states, the chemistry observed at extreme P-T conditions is radically different than that observed at ambient pressure and temperature. We seek to exploit the resulting novel chemistry to create new, stable materials with new functionality; understand the chemistry of planetary interiors; and facilitate the development of new theories with enhanced predictive powers.” And the Nov 2011 NNSA workshop on Basic Research Directions on User Science on the National Ignition Facility [37] identified the study of “Elements at Atomic Pressures” as providing “answers to fundamental questions about condensed matter and likely to reveal entirely new phenomena in materials”. The same report identified “Kilovolt Chemistry” as a priority direction and stated that at extreme compressions “new kinds of chemical phenomena are anticipated, with the participation in bonding of deep electronic levels.” [37].

These new states mostly exist (or are calculated to exist!) above 400 GPa, beyond the limit of static compression techniques [38]. They can thus *only* be accessed using ramp compression techniques, where a temporally-tailored laser pulse a few-ns in duration compresses the sample quasi-isentropically [39-41]. As a result, the sample stays very much cooler than in shock-compression experiments, and it remain in the solid phase to 400 GPa and above (see Fig 1b). Except for a few very recent studies at the Omega and NIF lasers in the US on diamond [40], *the behaviour of solid matter above 400 GPa remains completely unknown*.

Present ramp compression experiments are limited to several shots per year, and diffraction data are obtained from laser-induced x-ray backlighters [42]. But the quality of this diffraction data is on a par with that obtained in the first static-compression studies in the early 1960s, is very much poorer than that readily available with static compression techniques on synchrotrons such as Petra-III. By coupling a focussed kJ-scale laser driver with the ultra-high intensity x-rays from XFEL, the Helmholtz

Beamline would enter wholly unexplored regimes, and enable exceptionally high-quality diffraction data to be obtained. Achieving such data at pressures up to 1 TPa (10 Mbars) is an adventurous, but achievable goal. The shot rate would represent a several order of magnitude increase over current techniques, and would open this field from the realm of discovery, to systematic study, exploration and exploitation.

[1] "Connecting Quarks with the Cosmos," National Academies Press, 2003.
[2] "Frontiers in High Energy Density Physics," National Academies Press, 2003.
[3] LCLS: The First Experiments (www.slac.stanford.edu/pubs/slacreports/slac-r-611.html)
[4] The European X-ray Laser Project XFEL (http://xfel.desy.de)
[5] P. Patel et al., Phys. Rev. Lett. **91**, 125004 (2003) ;
[6] J. Rassuchine et al., Phys. Rev. E **79**, 036408 (2009).
[7] F. Perez et al., Phys. Rev. Lett. 114, 085001 (2010).
[8] M.S. Bakeman et al., in: Megagauss XI (conferences.theiet.org/mg-xi/mgxi-final-v7.0.pdf) p. 327
[9] Y. Sentoku et al, Phys. Plasmas **14**, 122701 (2007); L. Huang et al, in preparation.
[11] D.E. Fratanduono et al, J. Appl. Phys. **110**, 073110 (2011).
[12] See www.exoplanets.eu
[13] I. Baraffe, G. Chabrier, T. Barman, Rep. Progr. Phys. 73, 016901, 2010
[14] M. Morales et al., Proc. Natl. Acad. Sci. USA 107, 12799, 2010
[15] L. Caillabet, S. Mazevet, P. Loubeyre, Phys. Rev. B 83, 094101, 2011
[16] B. Holst, R. Redmer, M.P. Desjarlais, Phys. Rev. B 77, 184201, 2008
[17] W. Lorenzen, B. Holst, R. Redmer, Phys. Rev. B 82, 195107, 2010
[18] H.F. Wilson, B. Militzer, Astrophys. J. 745, 54, 2012
[19] J.J. Fortney, Science 305, 1414, 2004
[20] D.J. Stevenson, Space Sci. Rev. 152, 651, 2010
[21] G. Morard et al., High Energy Density Phys. 7, 141, 2011
[22] C. Cavazzoni et al., Science 283, 44, 1999
[23] M. French et al., Phys. Rev. B 79, 054107, 2009
[24] W. Lorenzen, B. Holst, R. Redmer, Phys. Rev. Lett. 102, 115701, 2009
[25] M. Morales et al., Proc. Natl. Acad. Sci. USA 106, 1324, 2009
[26] S.H. Glenzer, R. Redmer, Rev. Mod. Phys. 81, 1623, 2009
[27] F. Dorchies et al., Phys. Rev. Lett. 107, 245006, 2011
[28] M. Ross, High Pressure Equations of State: Theory and Applications, *High Pressure Chemistry, Biochemistry and Materials Science,* Acquafredda di Maratea, Italy (1993).
[29] M.I. McMahon and R.J. Nelmes, Chem. Soc. Rev., **35**, 943–963 (2006)
[30] J.B Neaton and N. W. Ashcroft, *Nature* **400**, 141 (1999).
[31] E. Gregoryanz *et al*, *Science* **320**, 1054 (2008);
[32] Y. Ma et al, *Nature* **458**, 182-185 (2009).
[33] E. Gregoryanz *et al*, Phys. Rev. Lett. **94**, 185502 (2005).
[34] C.L. Guillaume *et al*, Nature Physics **7**, 211(2011)
[35] C.J. Pickard and R.J. Needs, *Nature Mater.* **9,** 624 (2010).
[36] "Decadal Challenges for Predicting and Controlling Materials Performance in Extremes," (Santa Fe, 6-10.12.2009), http://www.lanl.gov/source/projects/marie/workshops.shtml
[37] "Basic Research Directions for User Science at the National Ignition Facility (NIF)." (Nov. 2011), http://nnsa.energy.gov/sites/default/files/nnsa/inlinefiles/nif_final_%20draft_100311_js_JH--high%20res.pdf
[38] M.I. McMahon, Top. Curr. Chem. 315, 69 (2011).
[39] R.F. Smith *et al*, Phys. Rev. Lett. 98, 065701 (2007).
[40] D.K. Bradley *et al*, Phys. Rev. Lett. 102, 075503 (2009).
[41] D.E. Fratanduono *et al*, J. Appl. Phys. 109, 123521 (2011).
[42] J.S. Wark *et al*, AIP Conf. Proc. 845, 286 (2006).

2.2 Ultra-High-Field Electrodynamics

The planned Helmholtz Beamline at the European XFEL offers new opportunities to test fundamental predictions of strong-field QED [1] and to search for new effects. The capabilities of the European

XFEL exceed those of LCLS in the relevant areas of photon energy, and the coupling to the ultra-intense PW lasers. We may imagine the quantum vacuum to contain, among others, virtual $e^{\pm}$ fluctuations, and we may seek to directly test the QED predictions concerning vacuum polarization. Precisely, the wording "vacuum polarization" means a change of the dielectric and magnetic susceptibilities due to an external Electromagnetic field. A prominent example is the propagation of a probe photon through the electromagnetic (quantum) vacuum. Similar to the propagation through a given material (e.g. a plasma), the probe photon may experience (i) dispersive modifications and changed polarization properties and (ii) absorptive effects, e.g. decay into a e^+e^- pair. These effects are interrelated by dispersion relations cutting rules, and the optical theorem. A variety of exciting possibilities for possible QED experiments at the European XFEL were discussed at the Dresden Workshop, but the most accessible for the first years of implementation of the Helmholtz Beamline are a proposed measurement of the “vacuum birefringence.” [1,2]

Vacuum birefringence

The experimental set-signature of vacuum birefringence consists of measuring the change of the polarization plane of the probe photon (XFEL) in the focal spot of high-field optical laser(s).[3] This is illustrated schematically in Fig. 1.

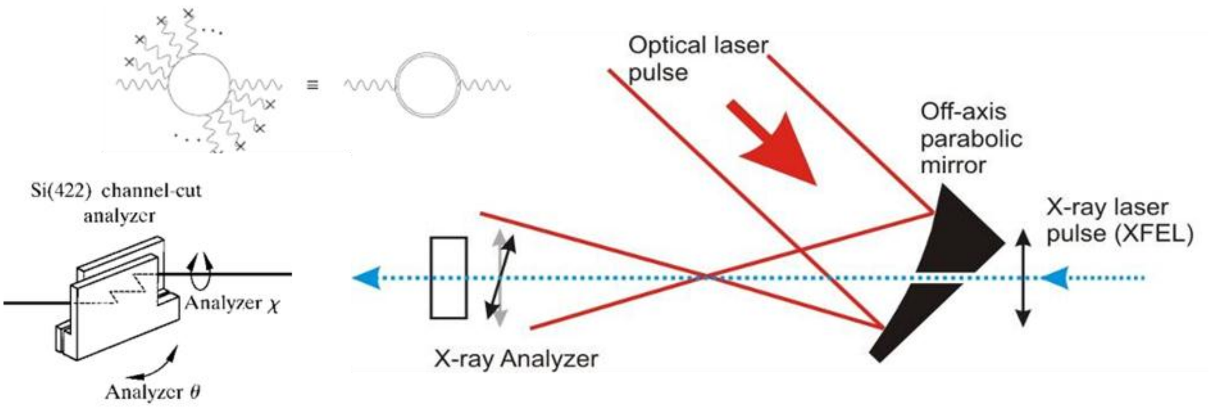

Figure 2.2.1: Proposed experimental test of QED predictions for vacuum polarization in strong external EM fields. Rotation of XFEL beam polarization is measured in PW-laser focus, with channel-cut Bragg analyzer.

The estimated ellipticity of the polarization plane of the probe photons (initially linearly polarized) in the laser focal spot of size d, [2] is

$$\delta^2 = 3.2 \times 10^5 \left[\left(\frac{d}{\mu m} \right) \epsilon^2 \nu \right]^2 ,$$

with $\epsilon = \omega_L a_0 / m$ and $\nu = \omega_{XFEL} / m$. This is based on the low-energy, low-intensity effective theory of QED, namely the Euler-Heisenberg Lagrangian describing direct photon-photon interactions. Another quantity is the rotation of the initially linearly polarized probe photon. The approximations leading to the Euler-Heisenberg effective theory descriptions are justified [3] for the envisaged XFEL-optical laser configurations. Spatial beam geometries are accounted for. Channel cut crystals [4] allow to measure the estimated effect which requires an extremely good polarization purity.[5] The quotation in Ref. [2] mentions the possibility to have access to the anomalous dispersion (i.e. the real parts of the two refraction indices become negative) which are related, via dispersion relations, to the imaginary part as a signal of pair production. Ref. [6] points out the promising opportunities of probing the quantum vacuum birefringence by phase contrast Fourier imaging.

Faraday rotation

A step towards the experimental verification of the vacuum birefringence is a measurement of the Faraday rotation of polarized XFEL photons in a plasma under the influence of a strong magnetic

(Cotton-Monton effect, magnetic birefringence) or laser field, which might be realized in ultra-intense laser-plasmas (e.g., Sec. 2.5). Reference [7] reports an enhancement of vacuum polarization effects in a cold collisional plasma. A detailed feasibility analysis of these effects is required to assess their ultimate viability for a possible experiment at the European XFEL.

[1] A. Di Piazza et al., arXiv:1111.3886, to be publ in Rev. Mod. Phys. cf. also Y.I. Salamin et al, Phys. Rept. 427, 41 (2006); M. Marklund et al. Rev. Mod. Phys. 78, 591 (2006).
[2] T. Heinzl, A. Ilderton, arXiv: 0811.1960.
[3] T. Heinzl, B. Liesfeld, K.U. Amthor, H. Schwoerer, R. Sauerbrey, A. Wipf, Opt. Commun. 267, 318 (2006).
[4] B. Marx et al, Optics Comm. 284, 915 (2011).
[5] I. Uschmann [talk at HZDR workshop 2011] reports a purity of $2.5x10^{-10}$.
[6] K. Homma, D. Habs, T. Tajima, Appl. Phys. B 104, 769 (2011).
[7] A. Di Piazza, K.Z. Hatsagortsyan, C.H. Keitel, Phys. Plamas 14, 032102 (2007).

2.3 Structural evolution of processes on atomic timescales

The study of ultrafast structural changes in physical and chemical processes is a major research area at x-ray FEL's. For example, the scientific motivations for using laser-driven shocks to study phenomena like materials strength and dislocation dynamics at high strain rate, elastic to plastic deformation, void nucleation and growth, and grain nucleation in liquid-solid phase transformations, are well documented, and will make extensive use of the 100-J class ns laser pulses of the Helmholtz-Beamline. The PW-class laser brings additional means to initiate dynamic processes, for example to use laser-accelerated ions to initiate damage cascades in materials, or possibly in the future to study structural changes in biomolecules in the presence of conventional irradiation and laser-generated ionizing radiation.

2.3.1 Dynamic response of Materials during particle irradiation

A predictive capability of processing and performance of materials under particle irradiation would have far reaching impact on the development of new materials and technologies, such as the design of electronic materials for advanced devices and for photovoltaics, or for the development of structural materials with improved high-temperature properties and high radiation resistance. It would moreover address a Grand Challenge [1] of materials science and engineering, This requires an excellent understanding of the dynamics and kinetics of atomic-scale features such as defects, foreign atoms, clusters, and their mutual interaction since the processes at the atomic level strongly influence the structural, thermal, mechanical, electronic, and magnetic properties of the materials. The unprecedented coherence and brilliance of the European XFEL beams will enable the study of just such atomistic effects [2-4], which can be initiated and investigated *in-situ* [5] with intense ps-beams of laser-accelerated-ions possible with PW-class lasers [6].

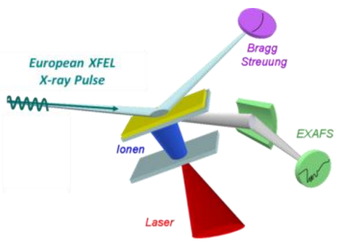

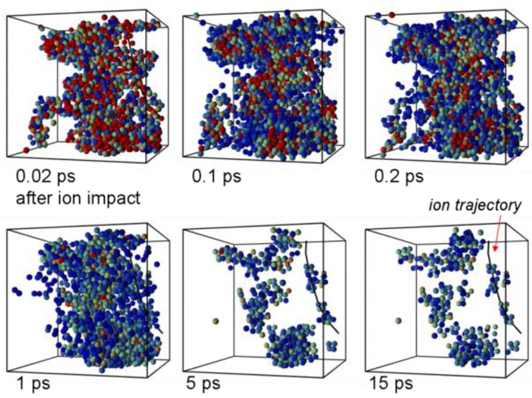

Figure 2.3.1:(a) Left: Schematic ion-pump XFEL-probe experiment (incl. XPCS, not shown). (b) Right: Molecular Dynamics simulations of damage cascades in Si, induced by Si recoil ions Refs. [7,8].

Figure 1 illustrates such an experiment to measure the time-history of a particle-induced collision cascade, with the goal of improving our theoretical understanding and validating Molecular Dynamics modeling. Key aspects include the initial distribution of recoils, the non-thermal collision cascade from each recoil ion, the thermalization of the kinetic energy in the local lattice leading to extended melt zones, the subsequent cooling and resolidification or recrystallization, the residual vacancies, interstitials and defect clusters, and their subsequent self-annealing. Extreme high doses can be reached, for which overlapping damage cascades may interact, leading to a different residual defect distribution (of either higher or lower concentration) depending on the degree of interaction of defect clusters or additional thermally induced annealing. The experiments will make use of a variety of scattering and spectroscopy techniques, including X-ray photon correlation spectroscopy XPCS (not shown) and diffuse scattering.

2.3.2 Functional Structural Radiobiology

One important scientific direction of the European XFEL is the pursuit of structural biology determinations of single large biomolecules and proteins in their native environment (without requiring protein crystallization). This will open to study the structural dynamics which are responsible for their function. Very recent data suggest that the membrane composition is importantly altered in cancer and that this has major implication on the function of proteins embedded in the membrane. One important potential application in Health Research could be to fundamentally understand the dynamics of inter-cellular signaling, which is controlled by the function of cell membrane proteins, and how these are triggered or changed during radiotherapy. (Recent studies in the Dresden OncoRay center have shown that an increase in intercellular signaling is responsible increasing the radiobiological resistance of 3D cell colonies by a factor of four, over that in single cell irradiation studies. Understanding and developing techniques to intervene in the cell membrane protein signaling process during radiotherapy could, in a longer perspective, have a profound impact on radiobiological research and eventually radio-oncology.)
The application of XFEL-based structure determination of biomolecules is expected to have a tremendous impact on the field of membrane protein research. These proteins are extremely difficult to crystallize for conventional x-ray analysis. Therefore, we will specifically explore the potential of monodisperse supramolecular assemblies as a platform for the study of membrane proteins using an XFEL. For this purpose, membrane-scaffolding proteins (msp) will be used to provide monodisperse patches of single molecules of membrane proteins in their natural cell membrane-like environment. The dynamics of membrane proteins is not assessable in crystals, where neither the native membrane nor conformational freedom is preserved. The envisaged platform technology will allow studying dynamic processes such as radical-induced radiation damage and transmembrane signaling in real time and in a large variety of oncologically relevant membrane proteins. This contrasts the situation in state of the art Cryo Electron Microscopy using computational reconstruction of such processes by statistical analyses of static snapshots. A pump-probe approach using the X-FEL in combination with synchronized laser sources for reaction induction will thus advance the field of biomolecular structural dynamics in an unprecedented way. Particularly its application to membrane proteins involved in cellular signaling will have a strong impact on modern pharmacology and radio-oncology, as mechanisms of drug action on large molecular complexes may be visualized with spatial resolution.

[1] Directing Matter and Energy: Five Challenges for Science and the Imagination. A Report from the Basic Energy Sciences Advisory Committee, Chair: John Hemminger, U.S. DoE, December 20, 2007. http://science.energy.gov/bes/news-and-resources/reports/basic-research-needs/
[2] A.M. Lindenberg, et al., Phys. Rev. Lett. **100**, 135502 (2008)
[3] M. Beye et al, Proc. Natl. Acad. Sci. USA **107**, 16775 (2010)
[4] M. Leitner et al., Nature Materials **8**, 717 (2009)
[5] A. Froideval et al.,J. Nucl. Mater. **416**, 242 (2011)
[6] P. Patel et al., Phys. Rev. Lett. **91**, 125004 (2003).

[7] K. Nordlund et al., Phys. Rev. B **57**, 7556, 1998
[8] M.J. Caturla et al., Journal of Nucl. Mat. **351,** 78, 2006

2.4 X-ray magnetic absorption and scattering in pulsed high fields

X-ray magnetic scattering in high magnetic fields at the European XFEL would allow for unique experiments at the forefront of condensed-matter physics. The available photon-wavelength range matches the requirements for investigations of rare-earth compounds comprising material classes such as pnictide- and cuprate-based high-temperature superconductors, strongly correlated electron systems, heavy-fermion materials, and spin-ice compounds with magnetic monopole excitations. Such experiments may be performed by means of rare earth K-edge XMCD. Among the rare-earth material classes, many compounds may be identified for exceptional studies to widen the present knowledge of condensed-matter physics.

Distinct from classical macroscopic measurement techniques, and even beyond capabilities of neutron diffraction methods, X-ray magnetic scattering experiments, comprising powerful techniques such as XANES and XMCD, will allow access to element selective information on band structure, spin, and orbital magnetic contributions. With such results, open questions concerning rare-earth valence fluctuations, spin-triplet admixtures to the superconducting ground state, and non-phonon mediated Cooper-pairing mechanisms for superconductivity may be answered. This will provide more insight in the microscopic electronic mechanisms and magnetic performance of many novel and functional material classes.

The access to quasi-static high magnetic fields has clearly advanced the understanding of high-temperature superconductors in the recent years. Pulsed-field techniques allow access to wide areas of their superconducting B-T phase diagrams. As an example, Shubnikov-de Haas oscillation experiments on high-quality samples performed in pulsed magnetic fields have given essential insight in microscopic electronic mechanisms of underdoped cuprate superconductors and have allowed for the determination of parts of their Fermi surface for the first time only several years ago [Doi 07, Hel 09] (cf Fig. 1). Doiron-Leyraud *et al* and others have observed particular quantum oscillations of the Hall resistance at high fields, e.g. in underdoped $YBa_2Cu_3O_{6.5}$ [Doi 07]. These quantum oscillations are indicative of the existence of electron pockets at the Fermi surface. However, so far ARPES experiments could not detect any of such electron pockets. High-magnetic fields have been found to have pronounced effects on the magnetic structure [Lak 02] and magnetic excitations [Cha 09] of cuprate high-temperature superconductors. Evidence for the existence of electronic anomalies is also supported by recent NMR experiments on $YBa_2Cu_3O_{6.54}$ in magnetic fields up to 28.5 Tesla [Wu 11].

In order to obtain an extended picture of the electronic ground state and nature of Cooper-pair condensation, high-field X-ray scattering experiments are required. The possible contribution of electron pockets at the Fermi surface as well as the role of the magnetic ground state and excitations to the Cooper pair binding process might then be studied in more detail. The challenging extreme sample and probe conditions for such X-ray scattering experiments may be provided with pulsed-field coils (t_{pulse} ~ 20 ms, B_{max} ~ 50 T), conventional ^{4}He-cooling techniques, and, in particular, with the exceptionally high x-ray intensity available at the XFEL. Only under such high magnetic fields ($B > B_c$), access to electronic structure and excitations in high-T_c superconductors is given as deeper in their superconducting state ($B << B_c$), quantum oscillations are no longer visible. In addition, high-filed magnetic X-ray scattering will allow for studies of the subtle interplay and balance of magnetism and superconductivity.

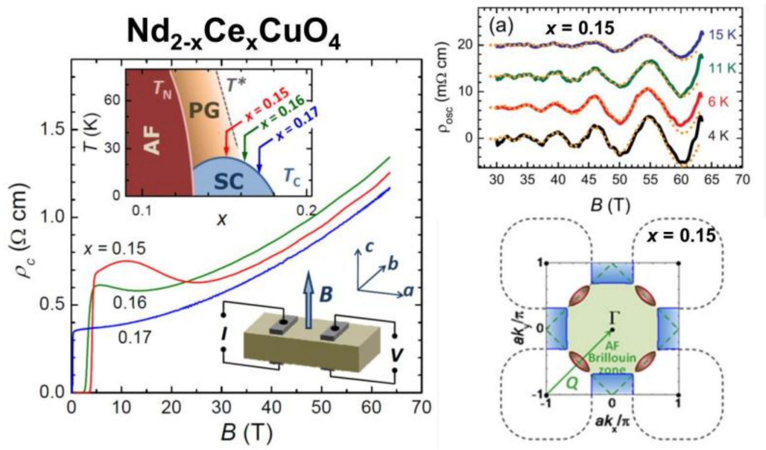

Fig. High-resolution quantum oscillation measurements performed in pulsed magnetic fields to about 60 T have been used in order to determine the Fermi surface of rare-earth based high-temperature superconductors (e.g. as $Nd_{2-x}Ce_xCuO_4$) as performed in a user experiment [Hel 09] at the Dresden High Magnetic Field Laboratory (HLD).

Relevant materials of such investigations are 4f-based cuprate (such as underdoped YBCO) and pnictide (such as REFeAs$O_{1-x}F_x$) superconductors as well. Such experiments require a wavelength in the 10^{-10} m range, and a diffractometer. The bunch pattern should be matched to the pulse duration of the magnet. By using one bunch train at XFEL with a duration of 600 micro seconds one could nicely cover the peak of the magnetic field with a duration of a few milliseconds. An energy band width of the order of 1% would be fully compatible with the experiment, too. A set of two pulsed field coils would allow for covering a wide range of experimental activities and challenges at high magnetic fields. The first type will provide the arrangement for an axial access of the photon beam through the magnet. The sample located in the center of the magnet bore (e.g. 20 mm) will be oriented to scatter the incident beam under a small angle. As a consequence, a classical magnet design with a straight-through bore might be chosen. Such types of magnets have been developed at the Hochfeld-Magnetlabor Dresden (HLD) at the HZDR for frequent use in its user facility. Fields up to 50 T at pulse duration of 10 to 30 msec might be achievable. Under that operation regime, a cooling and pulse-repetition time of the magnet of 10 to 20 minutes may be feasible. A considerable higher repetition rate (~ 1 pulse per min) will be possible at fields up to about 30 T. A liquid-N_2 cryostat will have to be used to get sufficient cooling of the magnet. The second type of magnet, a split-pair coil (Helmholtz-type geometry) will produce a magnetic field vertical to the incident beam. This setup will allow for scattering in the horizontal diffraction plane. The bore of that magnet (20 mm) will be designed sufficiently large to be able to insert a cryostat for sample cooling with x-ray transparent windows. These types of magnets may energized by a capacitive pulsed- power module as outlined in Chap. 3.6.

Further sample candidates for highlighting experiments will be given in spin-ice compounds such as $HoTi_2O_7$ or $DyTi_2O_7$ which show unique magnetic behavior comprising monopole-like magnetic excitations in consequence of their highly frustrated magnetic interactions between nearest and next- nearest neighbors [Cas 08]. X-ray magnetic scattering in high pulsed magnetic fields will provide element-selective magnetization data at fields where magnetic 4f-moments are progressively forced to magnetic saturation, i.e. at high magnetic field amplitudes which equal internal exchange fields. High-field X-ray magnetic scattering could also provide a direct access to crystal-electrical field (CEF) splitting and f-derived Fermi surface in many rare-earth based heavy-fermion compounds, such as $YbRh_2Si_2$ [Vya 10, Dan 11]. High-field XMCD, in particular, performed on systems, such as cubic Pr-based pnictides and chalcogenides where CEF energy level crossing may be forced by the exposure to strong pulsed magnetic fields would allow for a direct observation of Bose-Einstein condensation of higher excited (e.g. triplet) states in lower (e.g. singlet) ones.

[Doi 07] N. Doiron-Leyraud et al., Nature **447**, 565 (2007)
[Lak 02] B. Lake et al., Nature **415**, 299 (2002)
[Hel 09] T. Helm et al., Phys. Rev. Lett. 103, 157002 (2009)
[Cha 09] J. Chang et al., Phys. Rev. Lett. **102**, 177006 (2009)
[Wu 11] T. Wu et al., Nature **477**, 191 (2011)
[Cas 08] C. Castelnovo et al., **451**, 06433 (2008)
[Vya 10] D. Vyalikh et al., Phys. Rev. Lett. **105**, 237601 (2010)
[Dan 11] S. Danzenbächer et al., Phys. Rev. Lett. **107**, 267601 (2011))

2.5 Relativistic Laser-Solid Interaction Physics

The high brightness, polarization, and per-bunch photon intensity of the European XFEL, combined with the PW laser of the Helmholtz-Beamline, will provide revolutionary new capabilities for unraveling the extreme complexity of ultra-intense laser-solid-matter interactions. This will have a major impact on the entire field of relativistic laser-plasma physics, and an improved understanding of the fundamental laser-solid interaction will dramatically increase the scientific utilization of the many new PW-class lasers, and extreme-intensity laser facilities, being developed in world-wide. [1]

Ultra-intense, relativistic laser interactions with solid targets are widely studied for generating secondary particle beams and radiations (ions, electrons, positrons, neutrons, bremsstrahlung, EUV harmonics), for producing extreme states of matter, for studying magnetized-plasma phenomena of astrophysical interest, and for exploring the fast ignition concept for fusion energy. A critical aspect for experiments in each of these areas is the transport of huge current densities (>10^{13} A/cm^2) of relativistic laser-accelerated electrons, which is complicated by the return current dynamics, the dynamically changing ionization stage and temperature of the medium, strong resistive magnetic and electric fields, and the non-uniform temporal and spatial structure of the electrons accelerated from the laser absorption zone. For example, present state-of-the-art particle in cell (PIC) simulations predict the rapid development of two stream filamentation instabilities, rapid heating and large spatial gradients of the collisional resistivity, charge separation electric fields up to 10^{12} V/m, and the formation of quasi-static magnetic fields up to 500 MG near the laser focus, and of up to 100 MG resistive magnetic fields inside the solid density matter, as indicated in Fig. 1 (left).[2,3]

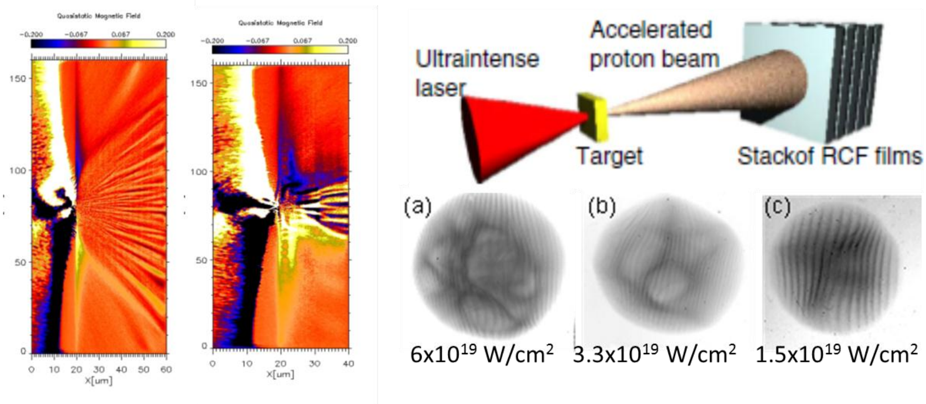

Figure. 2.5.1: (Left) PIC simulations of electron transport filamentation (quasi-static B fields) from relativistic laser interactions with Al target (left) and a layered Al/Au/Al target. Large quasi-static fields arise at material interfaces). (Right) Disruption of TNSA protons, from electron filamentation at high intensity [3].

Filamented electron transport can disrupt the quality of proton and ion beams accelerated by the TNSA mechanism (Fig. 1 right).[3-5] Recently, laser target size and specific shapes (e.g, micro-scale cones) have been shown to significantly affect the electron transport, causing a degree of localization and material heating (Fig. 2), through both the electrostatic [6] and quasi-static magnetic fields produced in the target.[7] Understanding the relativistic electron dynamics under these extreme conditions, including filamentation, transport, resistive modification, ionization dynamics, localization, and heating is presently one of the exceptional challenges in high-intensity laser physics.

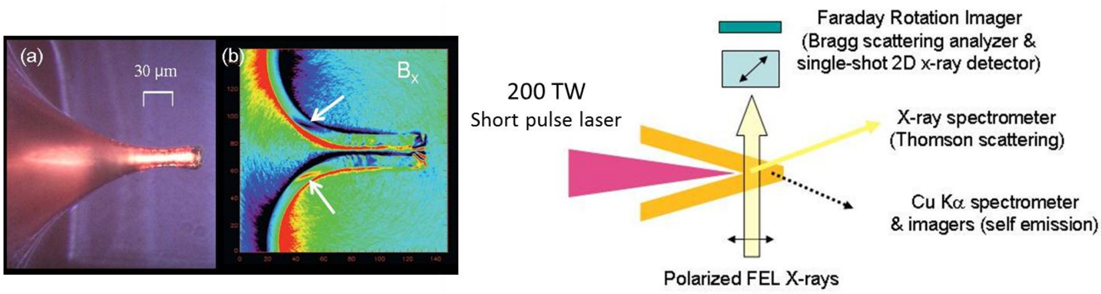

Figure 2.5.2. (a) Photo of free standing, 10 µm thick Cu cone (50 TW laser is incident from Left). (b) PIC simulation of quasistatic magnetic field after 1 ps (Arrows indicate resistive wall fields >10 MG). (c) Predicted energy density (temperature), showing enhanced, uniform heating in tip region.

At present, electron transport is usually deduced from characteristic x-ray self-emission imaging and spectroscopy. These are limited in both spatial and temporal resolution, and are correlated in a complex fashion with the hot electron relaxation physics. Probing with a high resolution narrow bandwidth XFEL beam would allow to directly measure the internal magnetic field structures in the solid-density target plasma by hard x-ray Faraday rotation.[8] Simultaneously, one could obtain Thomson scattering data (spatially averaged over the beam spot). Supplementing these with high precision absorption spectroscopy, using a percent bandwidth XFEL beam, would provide extremely high quality data, and allow to quantitatively understand how the electron transport dynamics behave at these extreme current densities, fields, and hot dense plasma conditions.

Hard x-ray polarimetry has improved significantly in recent years with channel-cut Bragg crystals ([9], Sec. 2.2), such that with the European XFEL operating in a self-seeded mode, the estimated signals are sufficient to obtain a high-contrast 2D Faraday image on a single shot (using an x-ray CCD camera as detector behind the x-ray analyzer). The Faraday rotation angle, given by the integral over the x-ray path length of the longitudinal magnetic field times the electron density:

$$\Delta\varphi \approx K\lambda^2 \int n_e B_z dz \qquad \text{(with } K = 2.629\times10^{-13} \text{ in M.K.S. units),}$$

suggests a 1 mrad polarization rotation, for a 50 MG field in solid density Ne-like Cu, viewed across a 20 µm chord length with 8 keV x-rays. This is well in excess of the available resolution with channel-cut crystals, and a single shot with high contrast, using a polarizer tuned to 3 mrad from full extinction.

[1] See ICUIL world map: http://www.icuil.org/events-a-activities/laser-labs.html
[2] Y. Sentoku et al, Phys. Rev. Lett. 90, 155001 (2003).
[3] Y. Sentoku et al, Phys. Rev. Lett. 107, 135005 (2011).
[4] P. Antici et al., *J. Phys.: Conf. Ser.* **244**, 022016 (2010).
[5] J. Metzkes et al, to be published.
[6] F. Perez et al., Phys. Rev. Lett. 114, 085001 (2010).
[7] J. Rassuchine *et al.*, Phys. Rev. E **79**, 036408 (2009).
[8] D.P. Siddons *et al.*, Phys. Rev. Lett. **64**, 1967 (1990).
[9] B. Marx et al, Optics Comm. **284**, 915 (2011).

3. Helmholtz-Beamline at the European XFEL – Technical Case

3.1 Overview

Realization of the strong scientific potential of combining high-power and ultra-intense lasers, and high-field magnets, with the XFEL will require specific technical requirements for the configuration of the SASE 2 Hall, modifications to the baseline HED Instrument, additional instrumentation, and additional high-quality laboratory space for the laser systems.

Due to lack of appropriate space in the XFEL Hall or Administration building, a new separate laser laboratory building must be built, and connected by a subterranean tunnel to the XFEL Hall for laser beam transport. This new building will also house the 1.5 MJ capacitor bank for the pulsed high-field magnets. It is foreseen to include additional required office space for the Helmholtz-Beamline operations staff, and of the researchers within the User Consortium. This can be coordinated with the needs of other User Consortia (e.g., EMBL).

The laser systems of the Helmholtz-Beamline must operate reliably as a User Facility, and must therefore be based on mature technology verified with operational prototypes. The ultra-intense laser system is planned to be either diode-laser-pumped Yb:CaF_2 (200 J in 150 fs pulses), or commercially developed Ti:Sapphire (30 J in 30 fs), depending upon the performance and reliability of two prototype systems at the time the technology decision must be taken. Both types of technology are presently under development (Figs. 1-2). Alternative technologies are under consideration for a 100-J laser with a shot-on-demand kJ-class capability, which will be addressed at an upcoming workshop.

The HED Instrument hutch requires radiation shielding commensurate with the ultra-intense laser operation (required already for the 100 TW system in the XFEL Baseline). A workable concept is presented with a cost estimate, based on heavy-concrete hutch walls and roof, with additional local shielding near the laser target. The radiation protection system and controls will need to be coordinated with the DESY Accelerator division. The HED Instrument will include connection to the PW and long-pulse laser systems, laser focusing optics, accommodation for compact pulsed coils, and additional laser- and magnet-specific instrumentation – all of which can be adapted from existing laser experiment facilities. A clean room must be sited in the SASE2 Hall for the PW-class vacuum compressor and associated laser diagnostics. A dedicated mobile 50 T high-field magnetic and associated x-ray diffraction detection system will be developed which can be moved into the XFEL beam.

The utility requirements for all components have been estimated, and are consistent with the SASE2 Hall design. Power and environment control for the lasers and field generators will be associated with the new building. Other requirements for the European XFEL include an additional temperature-stabilized synchronization-fiber-link to the laser laboratory (guided from the SASE2 Hall through the laser-transport tunnel), the option for self-seeding in SASE2, and an option for circular polarization for XMCD experiments.

3.2 PW-Class Laser Systems

The ultra-intense laser systems will largely be used for the generation of secondary particles and radiation for pumping and probing, and to create the strong-fields for QED experiments. For both of these, it is highly desirable to have a large pulse energy. For strong-field QED, this is important to maximize the birefringence signal using a high intensity pulse in a long Rayleigh length focus geometry. For unraveling the complexities of the ultra-intense laser-matter interaction, this would allow for example to split the PW beam into a main drive beam for the primary laser-solid interaction, with a 2^{nd} beam for proton deflectometry to probe the electric field structure, and a 3^{rd}

beam for XAS to probe ionization dynamics; while using the XFEL beam for Faraday rotation to image the magnetic field structure inside the solid density plasma.

For reasons of highest short-pulse energy at high reprate (~1 Hz) the first choice for the PW-class laser is a fully diode-pumped solid-state laser using a large bandwidth active medium. This class of laser architecture has been under development for some years, beginning with the POLARIS project at IOQ-Jena, and is presently being extended in the PENELOPE project at HZDR to Yb-doped CaF_2. This would have sufficient bandwidth to support pulses down to 150 fs, and simultaneously high pulse energy, of up to 200 J. It is fully diode pumped, and will be designed to operate at 1 Hz at the full energy level, corresponding to >1 PW. In addition, it can be operated at 10 Hz at the 200 TW level. The full operation prototype is planned for completion in 2015, and if successful, could meet the laser requirements of the Helmholtz Beamline at XFEL.

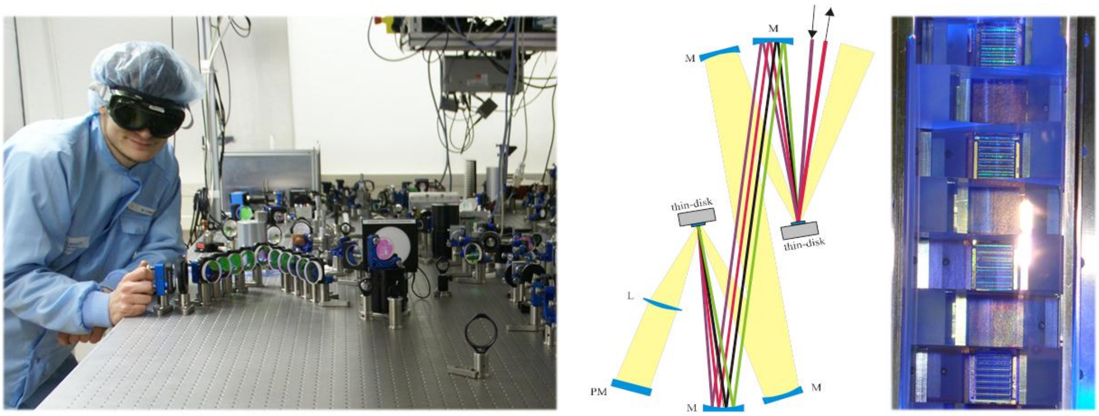

Fig 1: Development of diode laser pumped Yb:CaF2 short-pulse PW lasers (HZDR Penelope project). High efficiency is envisaged by multi-pass pumping and seeding low-gain disc amplifiers, requiring high brightness diode laser pump sources (Lastronics, right picture).

As emphasized above, it is essential that the Helmholtz-Beamline laser systems operate as a reliable User facility, to make best use of the extremely valuable XFEL beamtime. As a technology alternative "back-up", we are considering a PW laser based on Ti:Sapphire technology, which is developed commercially. There are presently two such systems in production, by Amplitude Technologies (DRACO upgrade at HZDR, Fig. 2), and by THALES (BELLA project at LBNL). Both will be installed in 2012, and are expected to be operational in 2013, which should provide a sufficient baseline of operational experience to establish either of these vendors as a reliable option.

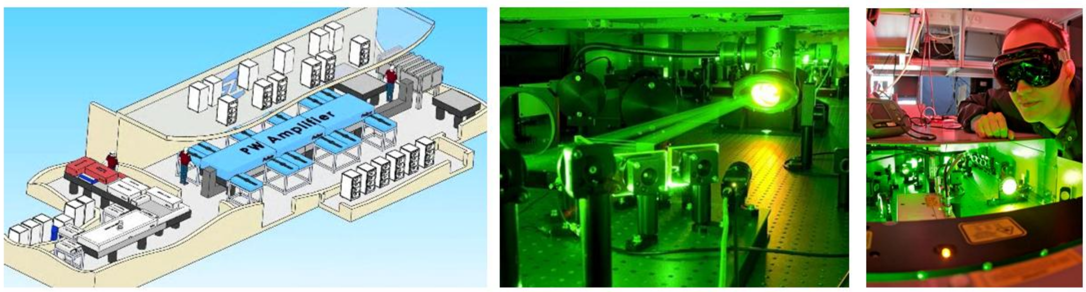

Fig.2: Sketch of the Draco-upgrade (HZDR) Ti:Sapphire PW laser design by Amplitude Technologies as well as impressions of the 6 J class cryogenic amplifier and front-end multipass amplifiers.

The PW-laser performance requirements must include high contrast (>10^{10}) and intensity (> 5 10^{21} W/cm2), with sufficient pulse shape, focal quality and shot-to-shot reproducibility for the planned experiments. The most demanding in terms of laser parameters are direct laser-solid interaction physics and the generation of secondary ion or high-harmonic beams from solids. The DRACO system (presently operating at 150 TW) has a similar principal use, primarily for solid-density interactions for laser-ion acceleration and for the study of matter under extreme conditions, and shares these requirements, as does the PENELOPE development. The THALES system has similar specifications, and its performance can be assessed in collaboration with LBNL.

The Helmholtz-Beamline lasers must be precisely synchronized to the XFEL beam pulses. This technology is being developed at both DESY, and in collaboration with DESY at HZDR. The latter makes use of the ELBE accelerator, which is based on the same 1.3 GHz superconducting TESLA cavities as XFEL, and includes the development of THz-based precision electron beam diagnostics. The DRACO and PENELOPE systems will both be synchronized to the ELBE accelerator bunches, and the technology solutions developed there will be adapted the final laser architecture chosen for the Helmholtz-Beamline systems. Therefore, within currently running projects at HZDR and DESY, and in collaboration with HI-Jena, most aspects of the both Ti:Sa and diode-pumped PW-class laser technology options, performance requirements, and coupling with and synchronization to the XFEL accelerator technology will be developed.

The technology choice for the PW-class laser system must be made in 2014 (ideally by end of 2013), for a desired installation and commissioning in 2015-16 at the Helmholtz-Beamline.

3.3 Long-Pulse Laser Systems

The few ns-pulse, 100 J high rep-rate and kJ-class shot-on-demand laser system is intended mainly for driving shocks in samples, and for cold, ramped-pulse quasi-isentropic compression. These address the scientific goals of bringing laser-driven shock and high-pressure experiments to the XFEL environment, in order to take advantage both of the unprecedented quality of the XFEL beams for probing, and the higher experiment shot rates, which promises to move this field from one of single-shot “discovery” physics, to systematic study.

The higher repetition rate for the experiments is in part realized by decoupling the shock or compression driver from the x-ray backlighter. In laser-only experiments, obtaining a sufficiently bright x-ray backlighter requires large laser energy (10’s of kJ) and complex target designs, with backlighter target foils close to, but appropriately shielded from the sample. Using XFEL as the primary x-ray probe fully removes these constraints, and will allow simpler geometries with allow an array of samples that can be arranged on a ladder, tape or target wheel, for rep-rated operation. One may also consider experiments in which a strong external magnetic field is applied to the compression sample, by means of pulsed coils (e.g., as a split Helmholtz-coil surrounding a target wheel). Reliable operation of in-vacuum 2D x-ray area detectors may require additional shielding against target debris or EMP. (This also to be considered for the PW laser.)

Both shock and quasi-isentropic compression experiments require shaped laser pulses of several ns duration. Precise pulse shaping has been developed at the LLNL NIF laser facility, using an active Mach-Zehnder interferometer to shape the seed pulse. It is foreseen to use this technique for the Helmholtz-Beamline compression driver.

High Reprate 100 J Laser

For a high-repetition rate, 100 J-class system, 1 Hz represents a safely achievable performance based on existing technology, and is a reasonable baseline. This can be achieved with fully diode-pumped technology, or with conventional flash-lamp pump lasers, driving a thermally-controlled amplifier.

Various suitable amplifier configurations are being developed, for example in the MERCURY project at LLNL, and DIPOLE at STFC. The back-cooled arrangement of the PENELOPE architecture could potentially also be adapted by replacing the CaF2 with YAG. The MERCURY, DIPOLE and PENELOPE prototypes are currently demonstrated at the 50 J, 10 J, and 1 J levels, respectively. The MERCURY and DIPOLE amplifiers are based on similar multi-slab geometries with active gas cooling between the slabs in an optimized laminar flow, either at ambient temperature or cryogenic. These can be scaled to 100 J or above by increasing the aperture, for which initial designs exist.

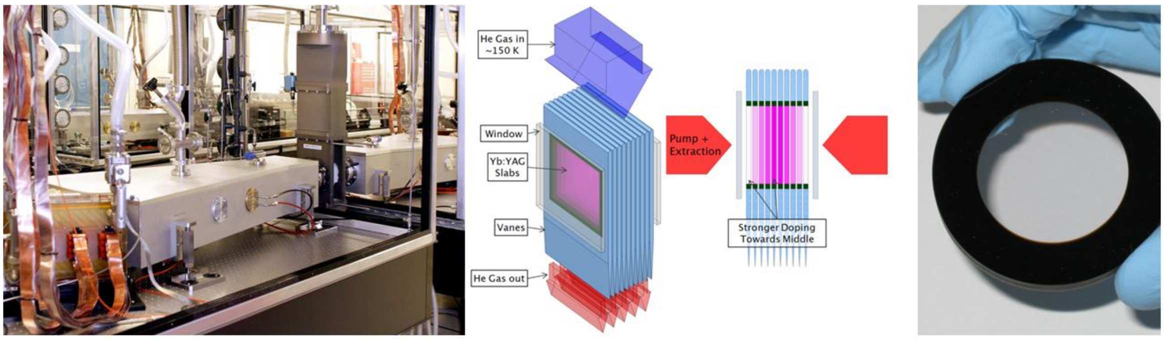

Fig 3: Picture of the diode pumped Mercury laser amplifier (LLNL) and a sketch illustrating its advanced gas cooling technique adapted for the STFC CLF Dipole project making further use of differently doped ceramic YAG amplifier slabs.

Shot-on-Demand kJ-class Laser

Scaling from the 10-50 J prototypes up to the kJ-class energy range at high reprate (few Hz) is a principal goal for the HiPER (STFC) and LIFE (LLNL) projects, and conceptual designs exist. These are diode-driven, however the system cost (based on presently available diode costs alone of ~10 M€) may be prohibitive. Since such rep-rated kJ-class systems are yet to be demonstrated--their actual performance and reliability are untested and difficult to predict with confidence. Significant advances would have to be made over the next two years in order for it to be considered for a user-facility like the Helmholtz-Beamline, but it remains in any case a future upgrade option.

An alternative near-term approach for high-energy compression experiments is to add to the 100 J system a booster amplifier at low-repetition “single-shot” operation. This would allow kJ-class operation for selected experiments at a reduced rep-rate. This booster could be flash-lamp pumped to reduce the initial expense. Conventional glass disk amplifiers are limited to the ~shot per hour range, due to thermal distortions. Designs exist for active water cooling, with up to the few shot-per-minute rate. Further investigation is needed to assess costs and reliability. This will be a topic at an upcoming workshop in April at GSI.

The “preferred technology” choice for the kJ-class system should be made in 2012, and will be incorporated into the funding plan. The power and facility requirements in the laser building suffice for a shot-on-demand kJ system.

3.4 Laser Transport

The Laser Building is presently planned to be 28 m from the SASE2 Hall, with a connecting underground tunnel. The 100 J and kJ long-pulse beams, and the uncompressed, 50 – 250 J PW laser beams, will need to be transported stably and at large aperture. Extremely stable transport is required for both pointing accuracy (with < 3 microrad stability), and path length (few micron overall, for precise synchronization with XFEL beam). This requires stability against vibration and thermal expansion. (The vibration requirements precluded the possibility of siting the laser in the laboratory space directly above the SASE2 Hall, due to building limitations.) The laser building will have a 1 m thick base to minimize vibration. The tunnel structure will be vibrationally isolated, so as to avoid coupling road noise to the turning mirrors at either end (Laser Building and SASE2 Hall, respectively).

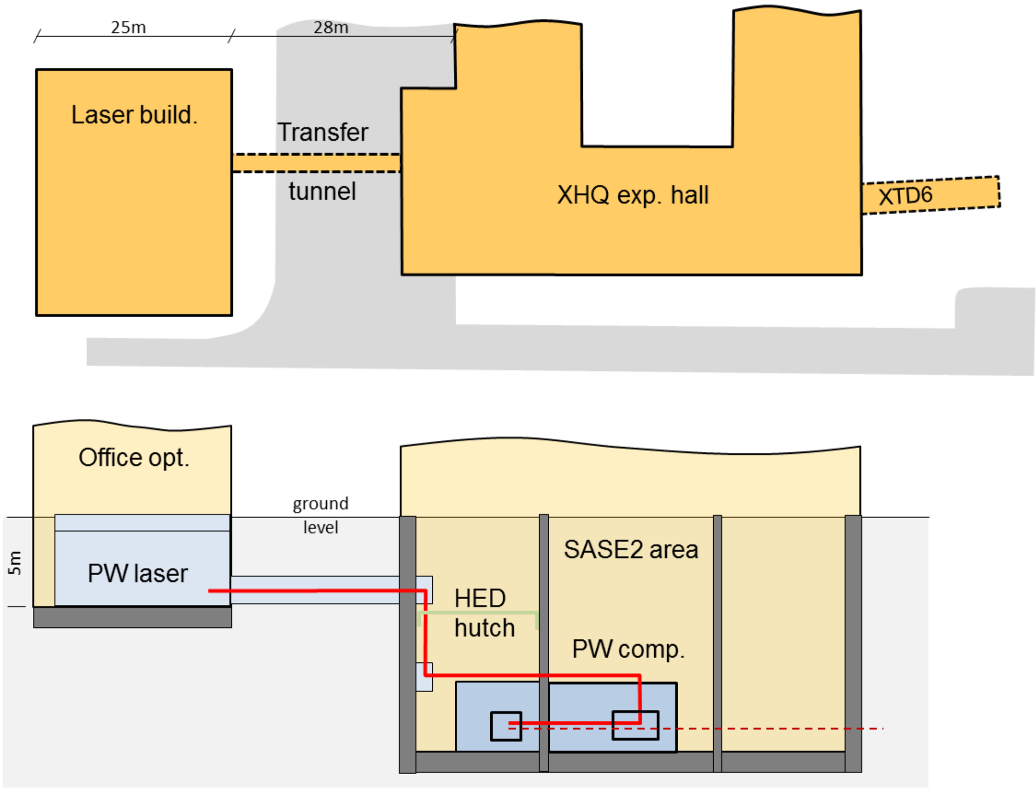

Fig. 4: Foot-print and cross-section of the SASE2 area of the XHQ hall and the proposed laser building.

These energetic beams require large aperture optics (30-50 cm diameter) to remain safely below the damage threshold, to assure long term reliability. The near field intensity distributions must also avoid diffraction extrema. We foresee using relay-imaging (with or without spatial filters), and sufficient beam transport diagnostics. To minimize vibrations, stable turning mirrors will be mounted at either end of the tunnel, with no active optical elements within the tunnel. An optional spatial filter, with large aperture may be included in the tunnel. The turning mirrors will be stably mounted respectively to the base of the laser building, and to the exterior wall of the SASE2 Hall. The beam will be transported from the turning box in the SASE2 Hall downwards, and then across the Hall above the Hutch roof to the PW Vacuum compressor in the Laser Clean Room. The long pulse beam will be transported to an optical table (either in the Laser Clean Room or directly in the Hutch), for diagnosis and if needed splitting, before being transported into the HED chamber. Additional lower energy probe beams will be either directly transported from the laser building through the tunnel with small aperture optical systems, or more likely be split off of the uncompressed PW beam in the Laser Clean Room.

The receiving mirrors in the Laser Clean Room and HED Hutch, will be built on stable towers from the Hall floor to minimize vibration. Active pointing systems will be employed for stabilization, with low-frequency feedback where appropriate to the turning mirrors, and higher frequency response by appropriately placed deformable mirrors. To reduce phase front distortion, the transport paths will be evacuated, where necessary. The final design of the laser transport system will involve experts from partner institutions, including GSI and LULI.

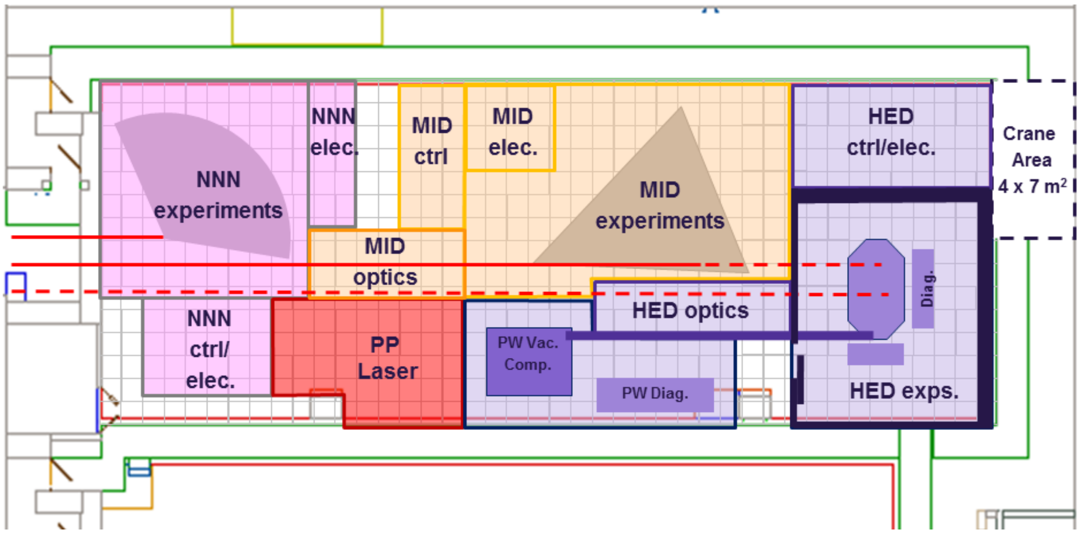

Fig. 5: Top view of the SASE2 experimental area. Space required for the HED hutch and high power laser installations (PW compressor) is marked in blue. Shielding requirements are indicated.

3.5 HED Chamber and Instrumentation

The detailed design of the HED target chamber, and the associated laser transport, focusing and diagnostics systems, must be developed in close collaboration with, yet under the direction of the HED Instrument Lead Scientist. There exists a broad base of experience to draw from within the membership of the User Consortium, including target areas at several lasers world-wide, operating in the kJ or PW range (mostly single-shot). The basic chamber design must accommodate multiple large aperture laser beams, space for beam folding, multiple focusing arrangements, flexibility for probing from above and around the equatorial plane, and space for in-vacuum and reentrant pulsed magnets. These are in addition to the essential XFEL-relevant requirements for specialized x-ray detectors and geometries for Bragg and Laue diffraction, diffuse scattering, large-angle Thomson scattering, Faraday rotation, XAS, XANES and other spectroscopic measurements.

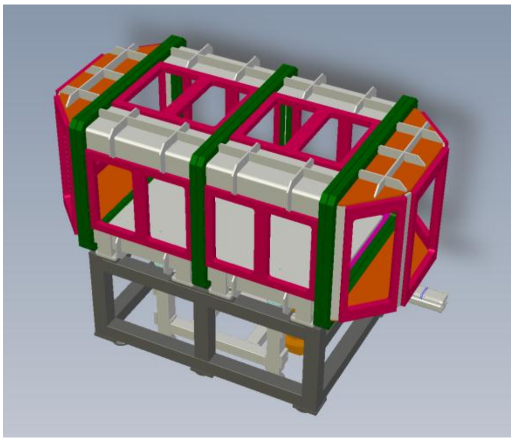

Fig. 6: Construction view of modular target chamber concept. The individual sections have a short-side dimension of 1 m, which is suitable to be maneuvered into the completed hutch and assembled in place.

The basic chamber architecture, whether monolithic or sectional, must be decided in 2012, in order to coordinate with the construction timeline of the shielding hutch. Depending on the design of the hutch roof, a monolithic chamber vacuum vessel may need to be installed before the final wall of the hutch is erected. Acceptable designs exist for modular chambers (see Fig. 6), which are fabricated and delivered in sections, which can then be maneuvered through the hutch door and assembled inside of the completed hutch.

There is a broad range of additional diagnostics required to realize the Helmholtz-Beamline scientific mission. These include:

Laser: pulse energy, near field, equivalent plane far field, spectrum, autocorrelation, ASE contrast, pointing, synchronization to RF, ramp-shape, focal spot size/shape/Strehl ratio.

Plasma self-emission: x-ray streak camera, x-ray imagers, x-ray spectometers, XUV and EUV spectrometers, single-hit X-ray CCD, THz spectrometer; optical streak camera.

Optical: 2ω, 3 ω probe beams, VISAR, SOP, FDI, optical Faraday rotation, interferometry

Particle: electron, proton, ion, positron spectrometers, Thomson parabolas, Bremsstrahlung spectrometer, neutron TOF detectors, ion TOF, Faraday cup arrays, proton imaging spectrometers

X-ray (XFEL): 2D area detectors, cooled x-ray single-hit spectrometers, hard x-ray polarimeters, dispersive crystal-based spectrometers.

High Pressure, Magnetism: diamond anvil cells (DACs), dynamic DAC, DAC laser heater, sample cryostats

XFEL instrumentation: x-ray split & delay, diamond phase plates, stabilized fiber-link for synchronization

Many of these instruments will be provided by External Contribution from the Partner Institutes. A preliminary list of instrumentation offered by the Consortium members includes:

CIW (Goncharov et al): Single-shot broadband optical, and Coherent Anti-Stokes Raman spectroscopy.
CELIA (Batani, Dorchies et al): Hot plasma and High Pressure diagnostics & expertise.
CLPU-Salamanca (Roso et al): UHV chamber and metrology; short-pulse laser expertise.
DESY (von Zimmerman et al): Beamline and high-magnetic field experiment infrastructure.
FZU-Prague (Korn et al): Laser-plasma diagnostics.
General Atomics (Stephens et al.): Target insertion technology; advanced target fabrication.
GFZ-Potsdam (Heinrich et al): X-ray scattering system (DAC), X-ray spectroscopy system (DAC).
IOP-CAS (Li et al): X-ray and spectrometers, electron & ion spectrometers; diagnostics; targets.
IOQ-Jena (Paulus, Uschmann et al): Channel-cut crystal hard x-ray polarimeters.
JIRT-RAS (Pikuz et al): crystal-based x-ray spectrometers with high spectral and spatial resolution; X-ray backlighting and X-ray microscopy components; crystal-based X-ray detectors.
KPSI (Bolton et al): Particle spectrometry, fast particle beam diagnostics; ultra-fast X-ray diagnostics.
Kyoto Univ. (Sakabe et al): Ultrafast electron diffraction system.
LBNL (Falcone et al): Spectrometer for inelastic x-ray scattering.
LLNL (Armstrong et al): High rep-rate 0.1 mJ high-pressure experiment capability using XFEL PP Laser.
LLNL (Hau-Reige et al): Contributions to X-ray Thomson scattering instrumentation and analysis.
LLNL (Shepherd et al): sub-ps X-ray Streak Camera.
LULI (Koenig et al): VISAR diagnostic. SOP diagnostic.
MBI-Berlin (Sandner et al): EUV spectrometer, Ion spectrometer, X-ray spectrometer.
MUT-Warsaw (Fiedorowicz et al): X-ray imaging system; high-energy laser system developments.
OSU (Freeman et al.): Compact Thomson parabolas for ions (pos. & neg.), positrons, & electrons.
Oxford Univ. (Wark/Gregori): Instrumentation for X-ray Thomson scattering and Spectroscopy.
SIOM (Li et al): Space- and time-resolved XUV spectrometer, high-resolution electron spectrometer.
SJTU (Sheng et al): X-ray spectrometers; THz spectrometers; Electron/Ion detectors; novel Targets.
Tata IFR (Kumar et al): Ultrafast dynamics and polarization measurement.
TU-Darmstadt (Roth et al): X-ray diagnostics; advanced laser targets; cryogenic laser targets.
TU-Dresden (Schroer et al): X-ray microscope; X-ray nano-focus system.
Univ. Bayreuth (Dubrovinsky et al): DAC's; internal laser heater (DAC); external E-field Pulser (DAC).
UC San Diego (Beg et al): Bremsstrahlung spectrometer; 2D Kα imager; HOPG spectrometer.
Univ. Frankfurt (Winkler et al): time-resolved laser fluorescence spectroscopy.
Univ. Pecs (Hebling et al): laser-based 1 mJ THz source.
Univ. Roma (Palumbo et al): Laser-proton diagnostics with associated data processing.
Univ. Siegen (Pietsch et al): Apparatus to apply high external electric fields to samples.
Univ. Stockholm (Haussermann et al): High-pressure experiment instrumentation.
Univ. Uppsala (Hajdu, Andreasson, et al): Sample injection system & related diagnostics.

3.5 Radiation Protection at the HED instrument Hutch

Compared to other X-ray hutches at XFEL, additional radiation shielding will be required around the HED Instrument because the particle and radiation beams that will be generated by the ultra-intense laser beams in the various experiments. The Hutch shielding and appropriate controls are designed to maintain the SASE2 Hall as an “open” non-radiological area, which requires a year-averaged effective dose of <1 mSv per year. In order to conservatively maintain these conditions outside of the HED Hutch, the shielding and walls must be designed to maintain an hourly-averaged dose well below 0.5 µSv/h (corresponding to a 2000 h worker year) for all operations. At continuous 10 Hz operation, this requires doses below 0.01 nSv/shot, or 0.1 nSv/shot at 1 Hz, outside of the Hutch. Higher per-shot yields may be allowed, with correspondingly reduced repetition rate. The Hutch will be equipped with active dose monitoring, in order to detect and stop any non-standard laser-target conditions, by inserting interlocked shutters into the upstream laser beam path. New experimental set-ups will require a dose verification survey, with a reduced number of shots, before allowing scale-up to the planned repetition rate. In no case will more than 0.5 µSv be produced outside of the Hutch in any one hour interval.

Source Terms

The relevant source terms for the radiation shielding calculations are taken from experimental configurations foreseen, and the simulations verified against existing high-intensity laser facilitiy operational data. Radiation conditions in excess of that from the XFEL beam itself, occur only for the ultra-intense (TW and higher) beams focused to above 10^{17} W/cm^2. This holds for applicaitions as proton or ion generation, isochoric heating, x-ray or high-harmonic generation from solids, or electron or betatron radiation generation from gas targets. The hard (penetrating) radiation primarily arises from the from the energetic electrons which escape the target, typically of order 1 – 10's nC. (The rapidly developing space charge potential as electrons leave the focal area, decelerates electrons generation later in the pulse.) At the available laser intensities, energies, and target conditions, the effective electron source terms are up to a few-10 nC of bunch charge, in a Maxwellian-like distribution with an average up to the relativistic ponderomotive limit of 10 MeV [Kluge, PRL 2012]. The use of thicker targets to create intense Bremsstrahlung environments must be considered on an individual basis to evaluate the per-shot dose rate and define the maximum allowable repetition rate accordingly.

FLUKA simulations have been performed to estimate the expect radiation fields and to design the hutch shielding walls. Approximately 40 – 80 cm of heavy-concrete is generally required in most directions. Additional local shielding near the target area, over the target area on the roof of the target chamber, and positioned as movable supplemental shield-walls in the forward direction with respect to a high-intensity short-pulse laser beam, are sufficient to meet the radiation dose limits. This is indicated in Fig. 7, which plots the total radiation field (dose) in µSv/hr, in and around the hutch for the highest expected routine operations. The simulation approach has been validated by a one-to-one comparison of predictions for the DRACO 150 TW laser in these configurations, to actual dose survey-data.

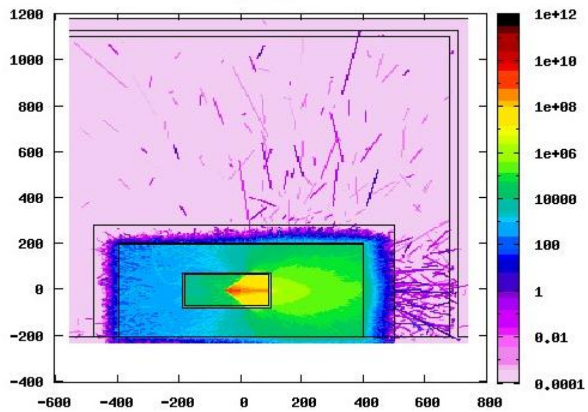

Fig. 7: Elevation view of simulated radiation field from high-reprate operation of the PW laser system. Hutch walls are from 40 – 80 thick heavy-concrete. Additional local shielding (5 cm Pb) above the target chamber, and at the chamber walls reduce the doses to acceptable levels.

The Figure shows a simulation of a standard-condition, high-rep rate experiment. The Hutch walls are 0.8 m thick heavy-concrete on two walls (towards which the most intense beams would be directed), and 0.4 m for the other two. An additional 1 cm thick Pb layer is included. The Hutch roof consists of 30 cm heavy concrete and 1 cm Pb, mounted on a steel girder frame. To save floor space, the entrance is by a rolling shield door, 30 cm thick. A 5 cm layer of Pb is placed on top of the target chamber for additional local shielding in the vertical direction.

3.6 High-Field Pulsed Magnet Systems

The high-field pulsed magnets will be driven by a 1.44 MJ, 24 kV, 40 kA pulse generation, developed by the High-field magnet Lab Dresden (HLD) at HZDR (Fig. 8). This will be located in the laser building, with the low inductance cables routed to the SASE2 Hall through the subterranean tunnel. The pulse generator will drive compact pulsed magnets of up to 50 T. A typical XMCD setup is shown in Fig. 8 from the ID12 beamline at ESRF. There, fields up to 30 T can be reached. The Helmholtz Beamline system will allow stronger fields (50 T), for few ms pulses. This is well matched to the 600 µs macro-pulse train, and should allow an entire B-field history in a single macropulse. The magnet/detector assembly fits on a 1 m table, which can be rolled and locked into position behind the HED target chamber inside the Hutch.

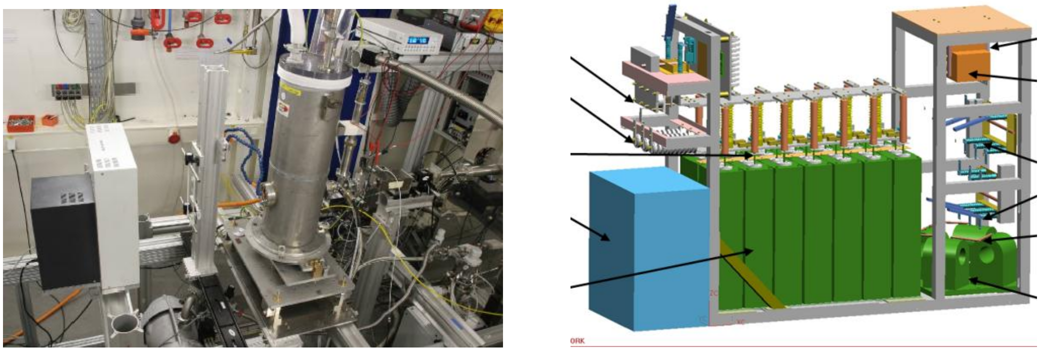

Fig. 8: Left: XMCD setup on ID12 at ESRF. X-ray beam comes from right. Cryo-cooled pulsed solenoid and IP detector with integrated reader on left.   Right: HZDR-HLD pulser module: 1.44 MJ, 24 kV. (4.2 m x 1.2 m).

3.7 Supplementary Laser Laboratory Building

Due to the shortage of sufficient space in the SASE2 Hall for the Helmholtz-Beamline laser systems, and due to the lack of sufficient vibration stability of the laboratory space above the Hall, a separate Laser Laboratory Building is required. For vibration stability this must have a thick foundation, and must be isolated from the surrounding roads, XVAC infrastructure, and the connecting tunnel. To minimize laser transport difficulties, the Laser Building is proposed to be positioned as close as possible to the SASE2 Hall, and connect by a below-ground tunnel with line of sight between laser turning boxes in the Laser Building and the external wall of the SASE2 Hall as sketched in Fig. 4.

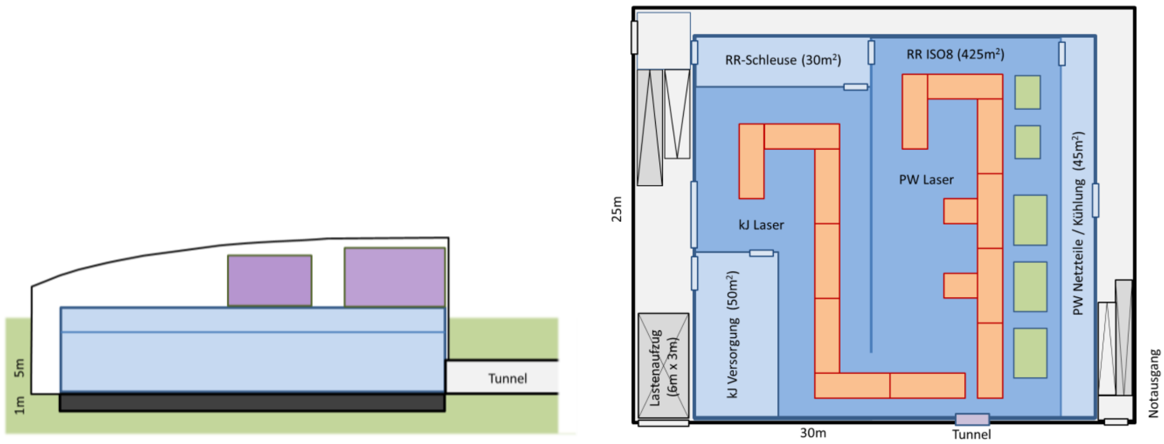

Fig. 9: Side view of the underground levels of the proposed laser building which does not yet incorporate additional office space in potential upper floors (left). Foot-print of the clean-room laser lab showing examples of PW and kJ laser table installations (right).

Figure 9 shows a preliminary design of the Laser Laboratory Building. It includes 600 m^2 of laser-clean room space, as well as place for the 1.5 MJ capacitor bank for the pulsed high-field magnets. The connecting tunnel is 5 m below ground and should be environmentally stable with the XFEL Hall. An area on top of the clean room was foreseen for technical installations and office space to accommodate the permanently-sited technical and scientific staff for the Helmholtz-Beamline. Additional office space will be required for the Helmholtz-Beamline Users, and potentially to scientists from other User Consortia (e.g., EMBL at XFEL). This could be accommodated by increasing the footprint or adding one or more additional office levels to this building.

The Laser Laboratory requirements for power and environment control have been specified. This building is separated from the XFEL Hall, to reduce impact on the XFEL construction schedule. Funding will be sought from BMBF and/or other sources. Construction should begin in 2014, in order to be completed before XFEL commissioning begins in 2015.

3.8 Coordination Issues with XFEL Commissioning

With the technical specifications as described in this chapter, it appears feasible to prepare, construct, install and commission the Helmholtz-Beamline with minimal impact on XFEL commissioning and operation. Certain major items should be completed during the construction phase of the XFEL Hall. These include: the swing crane, the Hutch shielding walls, the tunnel, and the support structure at the tunnel exit for the turning mirror boxes for the laser beam transport. These require relative heavy construction work, and should be completed before installation of the other instrument areas in the SASE2 Hall.

The Clean Room for the Vacuum Compressor can be a relatively straightforward modular construction. The Vacuum Compressor tank itself, as with the Target Chamber, can be made in a modular fashion, which allows to situate these after the Hutch and Clean Room are built. The Hutch roof should be designed for possible crane access. It would be sufficient to have an steel girder system which supports the main weight of the roof shielding, such that they need not be large-span (and hence quite heavy) self-supporting blocks. This must be designed and installed during the Hutch wall construction. With a modular chamber concept, each chamber section, as well as the other hardware, transport tubes, optical tables, and optics, could all be handled in the same way as any typical instrument system.

It is important to coordinate very soon with the DESY Accelerator group with regards to radiation protection strategy. All relevant procedures, standards and DESY site-specific policies must be followed for shielding design, personnel access system and interlocks.

3.9 Summary of Incremental costs for the Helmholtz-Beamline

Implementation of the Helmholtz-Beamline proposal for ultra-intense and high-power lasers and high-field magnets requires modifications in the SASE2 Hall layout and construction plan, and adds modest cost. This can be offset by the savings to the XFEL laser program, as the capabilities of the planned 100 TW laser for the HED Instrument can be provided (and vastly exceeded) by the Helmholtz-Beamline lasers. Note that some of these costs (ca. 400-500 k€ for Hutch shielding and Clean Room) would also have been required for 100 TW baseline laser system.

Estimated incremental construction costs:

Connecting Tunnel to Laser Building	200 k€
HED Hutch Shielding:	360 k€
Laser Clean-Room (PW Vacuum Compressor):	150 k€
Swing Crane (5 Ton) over HED Hutch:	30 k€
Subtotal	730 k€

Estimated incremental instrumentation costs (provided by XFEL):

Synchronization fiber link to Laser Building:	100 k€

4. Helmholtz-Beamline at the European XFEL – Project Plan

4.1 Overview

The realization of the Scientific and Technical Case for the Helmholtz-Beamline at the European XFEL will require close coordination with the XFEL construction, commissioning and operation. This is complicated by the absence of a firm funding commitment for the Helmholtz-Beamline project by the Helmholtz Association at the present time. This project is included in the Helmholtz Association roadmap for strategic Research Infrastructures (2011), with an intended start date in 2015. Ordinarily the Helmholtz Association approval process would result in a firm commitment first in 2014. It is therefore likely that certain initial stages of the project (e.g., shielding hutch and tunnel), must be constructed prior to a firm commitment. It is planned to develop an MOU between the HGF partners and XFEL, in order to mitigate the risk to the HED Baseline instrument, in the event full funding is not obtained.

This chapter summarizes the project plan, including schedule and costs, and yearly operation. The interrelationship with the HED Instrument is addressed. And risk minimization is discussed in the context of different funding scenarios.

4.2 Project Plan – Schedule and Budget Overview

The Table presents the time plan and budgets for the principal elements in the Helmholtz-Beamline project. The full project cost, including capital equipment and personnel, is estimated at 45.3M€, with an additional 12.5M€ contingency budget depending on options for the Laser Building and kJ laser compression driver.

The project personnel ramps up to 15 FTE's during the peak of the construction, with a 10 FTE steady-state staff during commissioning and operations. The estimated per-year operations budget is 2.5M€, for personnel and consumables (e.g., laser optics, large aperture gratings, experiment-dependent configuration changes such as new probe beams, etc.).

The major procurements of laser components and instrumentation, and development of custom laser and magnet systems, are scheduled to begin with the anticipated start of HGF funding in 2015. Commissioning of some sub-systems begins in mid-2016, and could be available for early experiments.

The Project Schedule indicates technology development and prototyping at HZDR, LBNL and elsewhere, up through 2014, which will provide the technical basis for the laser architecture decisions. These must be reached at latest in 2014/Q3 in order to assure timely delivery. The progress of these technology developments will be tracked throughout this period, to accelerate this decision point, if possible.

Between 4M€ to 6.5M€ of the project cost is anticipated to be incurred before the 2015 start of main HGF funding. This includes between 2.5M€ to 5M€ for the Laser Building, and 1.5M€ in additional costs for the transfer tunnel, hutch shielding, and the planning and design work required together with the HED Lead Scientist, for modifications to the HED baseline instrument to integrate the Helmholtz-Beamline capabilities. These are detailed in Sec. 4.3.

The Personnel and Magnet development through 2014, would involve existing experts in the partner Centers. Additional dedicated staff will be attached to the project during the construction phase, and a dedicated operations team will be resident at the XFEL site after commissioning. The operations team would be supported through HZDR and DESY, by the Helmholtz Program-Oriented Research (POF).

	2012		2013		2014		2015		2016		2017	2018...
Prototyping												
Installation Draco PW-HZDR (Amplitude Tech.)												
Installation BELLA PW-LBNL (Thales)												
Development DPSSL Penelope (HZDR)												
Installation Penelope (HZDR)												
Decision for PW class laser system @XFEL												
Manufacturing / Delivery (system dependent)							3000	3000	3000			
Installation and Comissioning										1500	500	
100J Laser manufacturing							1000	1000	1000			
kJ Laser manufacturing									3000	3000	4000	
Laser Operation, Maintenance												1500
Planning of laser building			100									
Construction of laser building				1000	1000	500						
Construction of laser tunnel					200							
Construction of beamline anchoring						150						
HED target area installation (shielding walls)						360						
Clean-room installation (PW compressor)							400					
Installation optical tables / laser labs							1500					
Fabricate vacuum chambers (target, comp)							500	1000				
Fabricate & Install beam line vacuum								400	400			
Large beam line optics ordering							500					
Large beam line installation									500			
Synchronization									500	500		
Pulsed magnet, supply, safety - design					100	100						
Pulsed magnet manufacturing							300	200	50	50	100	100
Pulsed power supply manufacturing							600	400	200			
Magnet & power supply safety installations								300	200			
HED Instrumentation							1000	1000	1000	1000	1000	100
Personnel (FTE)		1	2	2	3	3	12	12	15	14	10	8
Laser Development		1	1	1	2	2	7	7	6	6	2	
Laser Operations							2	2	6	6	7	7
Pulsed Magnet Development			1	1	1	1	2	2	2	1		
Pulsed Magnet Operations							1	1	1	1	1	1
Personnel costs (100kEuro x FTE)		50	100	100	150	150	600	600	750	700	1000	800
										Sum:	45310	2500
Contingency Laser Building				1000	1000	500						
Contingency kJ Laser									4000	3000	3000	
										Sum:	12500	

Table 4.1 Project Plan, including tasks, schedule, budget and personnel estimates, for the Helmholtz-Beamline at the European XFEL.

4.3 Pre-2015 Construction Requirements

These principal components which can affect the XFEL construction schedule in the SASE2 Hall involve the transfer tunnel, the HED hutch, and the infrastructure for the laser transport (turning-box towers). The construction of the Laser Building must also be coordinated in the plans for the outbuildings of the XFEL site.

As noted in the Technical Case, additional shielding is required for operation of any short-pulse lasers focused to intensities above several 10^{17} W/cm^2, due to the copious generation of energetic electrons in any solid, gas or plasma target. At the PW or 200 TW level, the shielding required is substantial, and should be included in the basic construction of the SASE2 Hall.

The Tunnel must also be included in the XFEL Hall construction. The turning mirror towers could, in principal be fabricated and installed later. However, since they are attached to the XFEL Hall, it is desirable to complete this during the heavy construction phase of the XFEL Hall completion.

The construction of the Laser Building must be coordinated with the overall XFEL site construction planning and scheduling, specifically with the other out-buildings. By separating the Laser Building from the XFEL Hall, the Laser Building development should not directly impact the XFEL development timeline. This offers additional flexibility in securing the full project funding.

4.4 Budget Options – Laser Building

The Laser Building cost is estimated between 2.5M€ to 5 M€, depending on size and features. The low-cost alternative is presented in Sec. 3.7, and is essentially a 600 m^2 high-ceilinged hall, in which modular laser laboratories would be constructed. Important is the 1 m thick foundation, for vibration stability. With air handling and utilities included, an estimated cost is 2.1M€ (600 m^2 at 3500 €/m^2).

The higher cost option is to include an additional 400 m^2 of office space (at ca. 2500€ / m^2). If built in multiple stories, this complicates the building design, and constrains the possible use of modular clean room construction. This would require higher construction costs to fully equip the laser laboratories (up to 5500 €/m^2) for an estimated cost of 4.3M€.

The final choice of building design should be made by end of 2012 or beginning of 2013. At which time it is hoped to have a clearer concept for the funding corridor.

4.6 Technical Impact on HED Baseline Instrument

The addition of the Helmholtz-Beamline to the HED Instrument creates additional requirements, beyond the baseline design. Already mentioned are the additional hutch shielding. In addition, the target chamber must be larger to accommodate the large aperture laser beams. The floor layout of the SASE2 Hall is affected: the hutch should be somewhat larger; and the laser clean-room on the Hall floor must accommodate the PW compressor, but not the 100 TW laser. An additional temperature-stabilized fiber-link synchronization station must be included and extended to the Laser Building.

Of these, the Target chamber design and the hutch shielding design must be established in advance of the anticipated funding commitment from HGF. If the Helmholtz-Beamline were then not ultimately funded, this would represent an unnecessary additional cost to the HED baseline instrument. Financial Risk Reduction is discussed in the next section.

It should be noted, however, that the inclusion of the heavier shielding to the HED Hutch allows an immediate extension of the science program of the HED Instrument, even in the case the Helmholtz-

Beamline were not fully funded. In particular, this would allow operation of the 100 TW laser, included in the Baseline, at full repetition rate and focused high intensity. Although this would fall far short of the capabilities of the PW-class system, some aspects of the Scientific Case would be at least partially enabled, including some research on relativistic laser-matter interactions, dynamic damage with laser-accelerated particles, and exploratory studies in strong-field physics.

As noted above, the 2012-2014 personnel components will be found within Center activities. This will include close collaboration with the HED Lead Scientist in the design for the Target chamber, and the design and construction of the Hutch.

We do not have at present a defined funding for the construction work prior to 2015. We would request the European XFEL if funding for the HED Baseline Instrument could be applied to the most time-critical items, namely the Tunnel and Hutch shielding. Also, we ask that the additional costs incurred for the enlarged Target chamber be covered initially by the HED Baseline instrument budget.

Once the commitment for Helmholtz-Beamline funding is secured, the supplementary costs of the Hutch and Tunnel can be immediately offset by financing the Target Chamber fully out of the Helmholtz Beamline budget.

4.6 Potential Funding Scenarios, and Risk Reduction

In the event that the Helmholtz-Beamline is not ultimately funded, the additional preparation costs incurred must be recovered. As well, any delay in the commissioning of the HED Instrument, due to the accommodation of the Helmholtz-Beamline, should be mitigated.

It is planned that the partner HGF centers will establish an MOU or a Research Contract with the European XFEL, to assure that in the event that the Helmholtz Beamline funding is not successful, the original capabilities of the HED Baseline Instrument will be assured. This will commit resources from the Centers' base programs.

The partner HGF centers are also pursuing the possibility of international contribution, which could help accelerate the process to obtaining a funding commitment from the Helmholtz Association.

In light of the above technical benefit that the enhanced hutch shielding will enable ultra-intense laser plasma physics at the HED Instrument, this will be included now as a defined scientific direction in the Helmholtz Research Area “Matter”, in the Program “From Matter to Materials and Life”, within the Program Topic, “Research with Highest Electromagnetic Fields.” This will have funding beginning with the POF III phase of the Helmholtz Funding, in 2015.